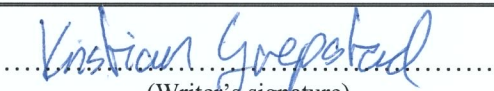
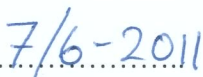




University of  
Stavanger

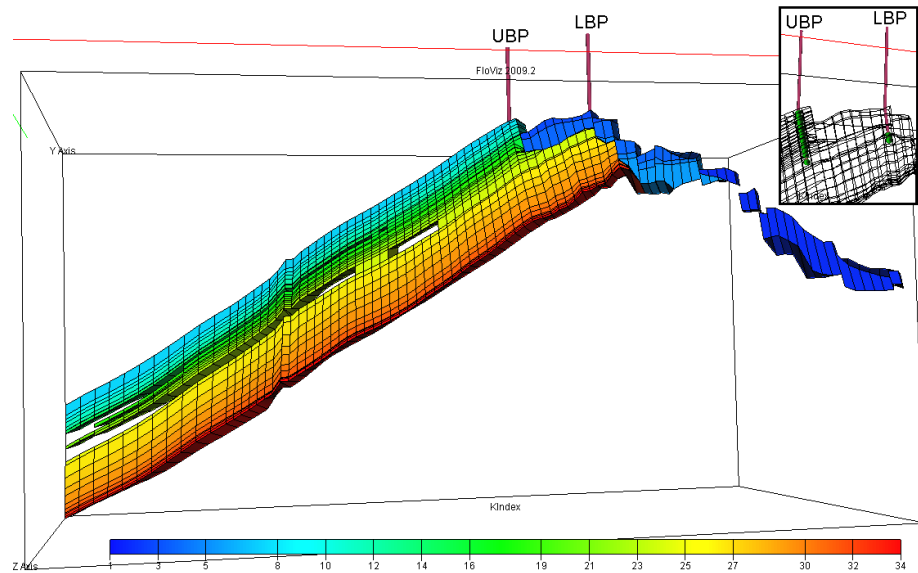
Faculty of Science and Technology

## MASTER'S THESIS

Study program/ Specialization: <b>MSc Petroleum Engineering / Reservoir Engineering</b>	Spring semester, 2011  <b>Open</b>
Writer: <b>Kristian Grepstad</b>	 (Writer's signature)
Faculty supervisor: <b>Jann Rune Ursin</b> External supervisor(s): <b>Kari Nordaas Kulkarni</b>	
Titel of thesis: <b>Upscaling of gas relative permeability during pressure depletion</b>	
Credits (ECTS): <b>30</b>	
Key words: <b>Modelling, upscaling, relative permeability, Statfjord.</b>	Pages: <b>82</b>  + enclosure: <b>11</b>  Stavanger,  Date/year



Master thesis:  
Upscaling of gas relative permeability during  
pressure depletion



Kristian Grepstad  
*University of Stavanger & Statoil ASA*

Spring 2011



### Acknowledgements

In making of this Master thesis there are several people I would like to express my gratitude towards. They have helped me in different ways with problems encountered, and through them I have been inspired.

First of all, gratitude goes to the University of Stavanger for giving me this opportunity and supporting me through my education. A great gratitude also goes to Statoil ASA, which has provided me with an encouraging, academic and social environment through the last two years of my education. Statoil ASA also helped me creating a good and challenging thesis, and providing me with office space and equipment.

My good friend, fellow student and colleague, Marthe Gilje Fosmark, has been a good support to have during the making of this thesis. We have worked with different theory and encountered different problems. However, through many discussions we have pushed each other to learn more and to explore the different views in the theory. In times of discouragement we have supported each other when writing our thesis.

Gratitude is also owed to Discipline Leader Res Tech, DPN OS SF PTC RP, Kari Nordaas Kulkarni, who is my mentor for this thesis and has made my work possible by inspiring me and guiding me through confusing times when struggling with the theory. Through interesting conversations and meetings she has tutored me, and without her I would not have been able to follow through.

A great thanks is also owed to Discipline Leader Petr Tech, DPN OS SF PTC RP, Øivind Fevang for posing the problem of the thesis to me, and helping me understand the theory through meetings and guidance.

Other persons who have earned my thanks when making this Master thesis, are all people working at Statfjord PTC, fellow student Pham Gia Minh, my friend Trond Håland and last, but not least, my loving family.

Statoil ASA/University of Stavanger - June 6, 2011  
Kristian Grepstad



## Abstract

Pressure depletion of an oil reservoir will result in release of dissolved gas when the bubble point of the oil is reached in the reservoir. This liberated gas will segregate upwards in the reservoir with low mobility until a vertical flow barrier is met by the gas. Liberated gas will accumulate below this barrier and create thin “layers” with high gas saturation, where the mobility of gas becomes high. These thin layers with high mobility will result in a relatively quick production of the liberated gas compared to “thick” layers used in conventional reservoir simulation grid, with low average gas saturation.

In order to simulate this effect more accurately, a method for upscaling the relative permeability and critical gas saturation is proposed in this thesis. Through simulation and analysis of the results it can be established a method of upscaling a 2D reservoir simulation model. However, without further simulation and analysis of a 3D scenario, it is not possible to establish if the method is adequate in a 3D scenario. All conclusions made in this thesis are considered for a 2D simulation model only. However, for the Statfjord Field, which is investigated in this thesis, it is still reasonable to assume that a 3D upscaling would be quite similar, assuming linear flow towards the top of the structure. The assumption of linear flow towards the top of the structure is based on observations of former injected gas with tracers.

Conventional simulation grid is observed to underestimate the gas production when gas is liberated in the reservoir. The recommendations presented, in order to include the effect, is divided into two different cases in this thesis; recommendations when creating a new reservoir simulation model and recommendations when upscaling an already existing reservoir simulation model.

If a simulation model is to be created, an adequately thin layer created below a vertical flow barrier will make ECLIPSE able to simulate the effect of gas creating a high mobility layer. The thickness of the layer must be evaluated in each separate situation, depending on the amount of liberated gas expected.

If a reservoir simulation model already exists, an upscaling method is a more practical approach. A small area which is representative for a larger region is chosen. Layers located below a vertical flow barrier are refined into adequately thin layers, and a transmissibility weighted average relative gas permeability is calculated and plotted against pore volume weighted average gas saturation. A Corey relative gas permeability is adapted as a best match by varying the Corey exponent and critical gas saturation. The Corey relative permeability tables and critical gas saturations found are assigned to the original layer, which was refined, as upscaled parameters. If the area chosen for upscaling is representative for a larger region,

the upscaled parameters can be assigned in the respective layers in the larger region.

Reservoir simulation models studied in this thesis originates from the full field reservoir simulation model of the Statfjord Field. Analyzing the upscaled simulation model indicates a significant increase in total cumulative gas production, as high as 7 % through the period investigated. This may affect the estimated gas reserves in the Statfjord Field, and is of great importance in an economical aspect.



---

## Contents

<b>1</b>	<b>Introduction</b>	<b>1</b>
1.1	Motivation . . . . .	1
1.2	The Statfjord Field . . . . .	3
1.2.1	Field Structure . . . . .	3
1.2.2	Depositional History . . . . .	5
1.2.3	Source rocks and migration paths . . . . .	8
1.2.4	Statfjord Late Life (SFLL) . . . . .	9
1.3	Reservoir simulation . . . . .	12
1.3.1	Reservoir simulation study . . . . .	12
1.3.2	Black Oil Model . . . . .	13
1.3.3	Input Data . . . . .	14
1.3.4	Reservoir Simulator . . . . .	19
1.3.5	Post processing software . . . . .	20
1.4	Upscaling . . . . .	22
<b>2</b>	<b>Building an applicable model</b>	<b>25</b>
2.1	Grid and input parameters exported from FFM2005 . . . . .	25
2.2	Preparing the model for ECLIPSE . . . . .	26
2.3	Adapting pressure development . . . . .	27
<b>3</b>	<b>BASE CASE</b>	<b>29</b>
3.1	Focus of comparison . . . . .	29
3.2	Simulation results . . . . .	29
<b>4</b>	<b>Base Case with refined East Flank grid (BASE CASE REF)</b>	<b>33</b>
4.1	Modification . . . . .	33
4.1.1	RESVIEW divide command . . . . .	34
4.2	Simulation results . . . . .	35
<b>5</b>	<b>Refined Main Field grid (RMF 1)</b>	<b>39</b>
5.1	Modification . . . . .	39
5.2	Simulation results . . . . .	41
<b>6</b>	<b>Refined Main Field grid (RMF 2)</b>	<b>47</b>
6.1	Modification . . . . .	47
6.2	Simulation results . . . . .	49
<b>7</b>	<b>Number of layers below vertical flow barriers</b>	<b>53</b>
7.1	Modification . . . . .	53
7.1.1	Three thin layers below vertical flow barrier (SENS 3) . . . . .	53

## CONTENTS

---

7.1.2	Two thin layers below vertical flow barrier (SENS 2) . . . . .	55
7.1.3	One thin layer below vertical flow barrier (SENS 1) . . . . .	55
7.2	Simulation results . . . . .	55
<b>8</b>	<b>Upscaling relative gas permeability and critical gas saturation in Main Field</b>	<b>59</b>
<b>9</b>	<b>BASE CASE REF with upscaled parameters in Main Field (BASE CASE REF UPSC)</b>	<b>63</b>
9.1	Modification . . . . .	63
9.2	Simulation results . . . . .	63
<b>10</b>	<b>Further work</b>	<b>67</b>
<b>11</b>	<b>Conclusion</b>	<b>69</b>
11.1	Recommendation when building a new reservoir simulation model	69
11.2	Upscaling an existing simulation model . . . . .	70
11.3	FFM2005 . . . . .	70
	<b>References</b>	<b>73</b>
	<b>Appendix</b>	<b>75</b>
A	Figures and Tables	75
B	Example of an ECLIPSE *.DATA file	83

# 1 Introduction

## 1.1 Motivation

The Statfjord Field has been producing hydrocarbons since 1979, but has passed its days with high oil production rates and it is beginning to be challenging to drain further. With focus on recovery, the final phase of production started in 2007 with the aim of extending the life of the field. The project is called THE STATFJORD LATE LIFE (SFLL)[14], and is expected to extend the production of the field from 2009 until 2020. In contrast to earlier pressure maintenance by water and gas injection, the objective of SFLL is a pressure depletion of the reservoir to liberate dissolved gas, turning it into a gas field [2]. This strategy is expected to increase the recovery of both oil and gas. Recovery of oil and gas by the end of 2010 is estimated to 65,5 % and 54 % respectively, and expected increased to 66 % and 68 % in 2020 [6]. The expected recovery of gas involves great uncertainties, and is an important subject of closer investigation. The STATFJORD RESERVOIR DEVELOPMENT PLAN 2007[14] suggests an expected gas recovery of 72 % in 2020, while this number has been decreased to 68 % in the ANNUAL STATUS REPORT 2010 FOR STATFJORD FIELD[6]. This decrease is caused by changes in the relative gas permeability in the simulation model for the Statfjord field, and implies the importance of understanding the flow of released gas and its impact on drainage.

The hypothesis is that the liberated gas might flow vertically with low mobility until it meets a vertical flow barrier/restriction where the gas will form thin “layers” with high mobility. These high mobility layers will lead to a relatively quick production of the liberated gas compared to “thick” layers with low gas saturation as in conventional reservoir simulation grid with rock relative permeability curves. In the view of this idea, the impact on the reservoir model must be evaluated with respect to grid size and upscaling. The aim is to develop upscaling methods for relative permeability.

Gas liberated from oil when depleting the Statfjord Field is mainly expected in the BRENT GP. The main focus of this thesis will therefore be the BRENT GP. of the Statfjord field. When investigating effects, a slice of the FFM2005, Statfjord Full Field Simulation Model, is considered in order to investigate a model with realistic properties.

This thesis will divide the analysis of the result into two parts:

- How to upscale an already existing simulation model to include the effect of thin, high gas mobility layers.
- How to include the effect of thin, high gas mobility layers when building a new model.

The expected result of including this effect in a reservoir simulation model is that gas production will increase, with earlier mobile gas phase and higher production rates.

An introduction and explanation of the Statfjord Field structure and layout is first presented, followed by some basic theory. The basis for the created

## ***1 INTRODUCTION***

---

model of investigation is then presented, followed by different modifications of that model. Analysis of the different scenarios and simulation results creates the basis for the conclusions drawn in this thesis.

## 1.2 The Statfjord Field

About 200 km northwest of Bergen, on the western side of the North Viking Graben, the Statfjord Field is located in the Norwegian blocks 33/12 and 33/9 and enters the UK block 211/25. A geographical view is presented in Figure 1.1. Mobil Exploration Norway INC discovered the field when drilling the wild-cat well 33/12-1 in 1973 [3], which penetrated the Brent, Cook and Statfjord reservoirs. Oil was found in the Brent Group sandstone of mid-Jurassic age and production started in 1979. Statoil became operator of the field on January 1, 1987. A final settlement for the division of the field was established in 1997, dividing the Statfjord Field into 85.46869 % Norwegian and 14.53131 % British.

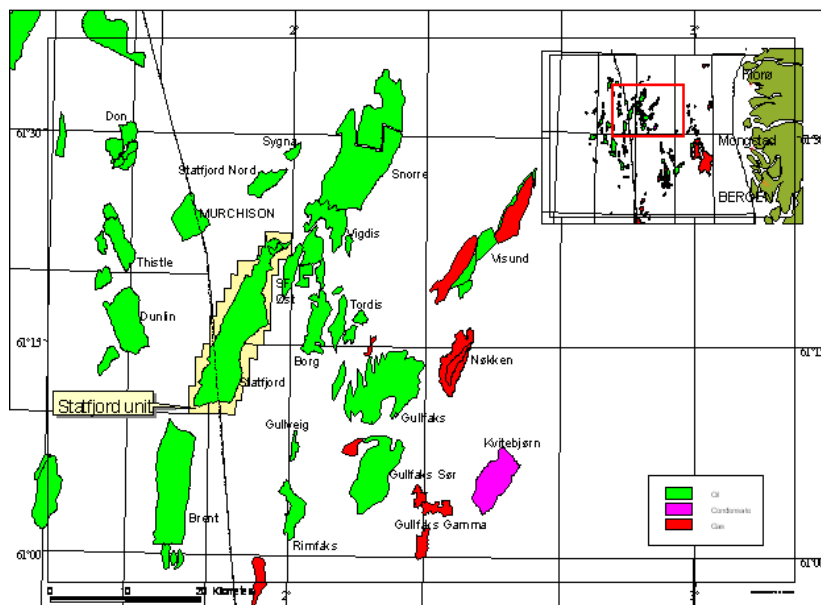


Figure 1.1: A geographical view of the Statfjord Field [6]

### 1.2.1 Field Structure

In terms of oil reserves, the Statfjord Field is the largest discovery in the North Sea, and one of the oldest producing fields on the Norwegian continental shelf. The oil zone covers an area of approximately 26 x 5 km. It is situated on the western margin of the North Sea Rift System on the foot wall of one of the major faults of the North Viking Graben, and on the crest of a SW-NE trending tilted fault block.

The field can be divided in a relatively uniform MAIN FIELD fault block, dipping approximately 6-7°, on the western side of steep normal cross-faults, with an EAST FLANK gravitational collapse zone, heavily deformed by rotational block slides along the Main Fault scarp, on the eastern side. The MAIN

## 1 INTRODUCTION

---

FIELD reservoirs consist of sandstones ranging in age from Late Triassic-Mid Jurassic. The EAST FLANK holds reworked sandstones from the Mid-Upper Jurassic layers [14]. A geological cross section of the MAIN FIELD and EAST FLANK is shown in Figure 1.2.

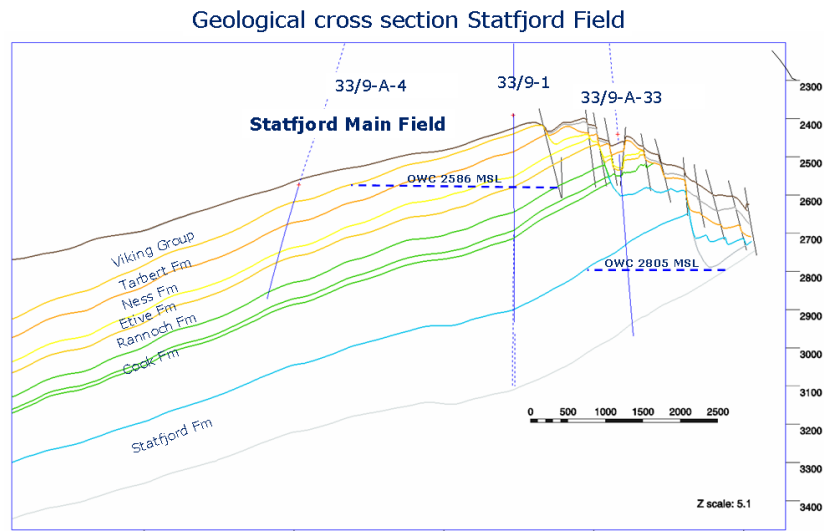


Figure 1.2: Geological cross section of the Statfjord Field[14]

Lithostratigraphically the Statfjord Field is divided into VIKING GP., BRENT GP., DUNLIN GP. and STATFJORD FM. A detailed lithographic overview of the Statfjord Field is presented in Figure A.1 on page 75. The shale dominated DUNLIN GP. separates the two main reservoir units, STATFJORD FM. and BRENT GP., which both possess excellent reservoir qualities and are found at depths ranging from 2300 to 3000 m. The VIKING GP. is situated on top of BRENT GP. and contains mostly shale in the MAIN FIELD, while in the EAST FLANK it also contains the reservoir sandstone REWORKED BRENT. The conceptual model is shown in Figure 1.3, and some important reservoir parameters for the BRENT GP. and STATFJORD FM. are presented in Table 1.1.

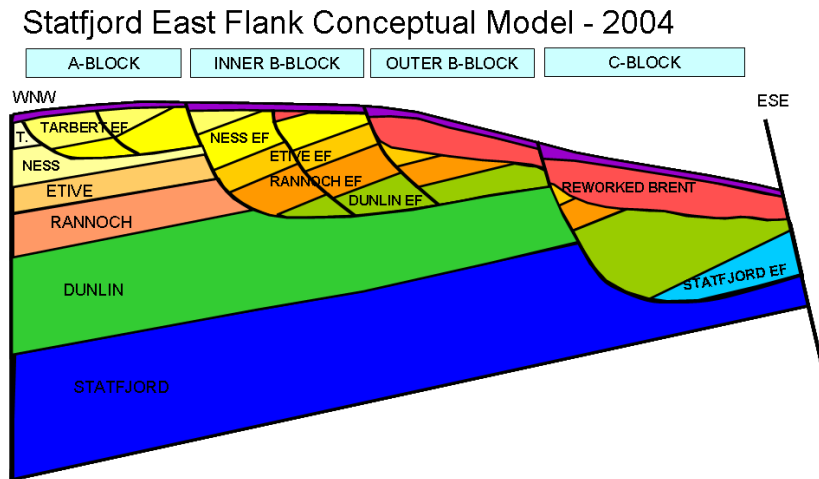


Figure 1.3: Statfjord East Flank conceptual model [14].

Parameter	BRENT GP.	STATFJORD FM.
Datum depth	2469.0 m	2710.0 m
Initial pressure	383.4 bar	404.3 bar
Initial reservoir temperature	88.9 °C	96.7 °C
Initial WOC (TVD MSL)	2586.3 m	2830/2814/2806 m
Bubble-point pressure	270.0 bar	200.0 bar
GOR	185.0 Sm <sup>3</sup> /Sm <sup>3</sup>	156.6 Sm <sup>3</sup> /Sm <sup>3</sup>
Oil viscosity	0.37 mPa·s	0.36 mPa·s
Oil gradient	0.0645 bar/m	0.0655 bar/m
Oil FVF	1.53 m <sup>3</sup> /Sm <sup>3</sup>	1.47 m <sup>3</sup> /Sm <sup>3</sup>
Critical gas saturation	6.2 %	6.2 %
Water compressibility	4.002·10 <sup>-5</sup> bar <sup>-1</sup>	4.785·10 <sup>-5</sup> bar <sup>-1</sup>
Rock compressibility	4.120·10 <sup>-5</sup> bar <sup>-1</sup>	4.34·10 <sup>-5</sup> bar <sup>-1</sup>
Aquifer/HCPV volume ratio	9	18

Table 1.1: Reservoir parameters for the BRENT GP. and the STATFJORD FM.[4]

### 1.2.2 Depositional History

This whole subsection is in large parts inspired from [14] and [15].

The deposition of the reservoir section in the Statfjord area is bounded by two main tectonics phases, the Early and Late Cimmerian rift phase. The North Viking Graben opened as a result from the first rift phase occurring in the Permian-Triassic (250 mya). The HEGRE GP. was deposited during Mid-Late Triassic as wedges were built out as fans and alluvial plains into terminal flood basin lakes and brackish flood basins.

**Statfjord Fm.** The base of STATFJORD FM. is defined as the top of the 20-30 m thick fining upwards shale sequence in HEGRE GP. It was deposited in Late Triassic - Early Jurassic, and was dominated by a southerly dipping continental palaeoslope going to shallow marine environments in the south. Overall deposition is defined in a structurally intra-continental depression set up by thermal driven post-rift subsidence oriented N-S, receiving supply from north-west and north-east directions. The STATFJORD FM. consists of RAUDE MB. (Lower Statfjord, LS), EIRIKSSON MB. and NANSEN MB. (Upper Statfjord, US). Lower Statfjord is dominated by repeated successions of braided stream deposits overlain with floodplain claystones, but consists of more connected sandstones moving towards Upper Statfjord. The deposition in Upper Statfjord is mainly sandstone, with more than 80 % sandstone with good vertical and horizontal connectivity in EIRIKSSON MB., and transgressive trend is dominating towards a shore face in NANSEN MB.

**Dunlin Gp.** The DUNLIN GP. consists of AMUNDSEN FM., BURTON FM., COOK FM. and DRAKE FM., in this order moving upwards. The continental environment found in the STATFJORD FM. is terminated in form of transgression and marine environment defining the boundary to the DUNLIN GP., and happened at a fast pace (in a geological point of view) over at relatively flat topography. This becomes evident by no inter fingering with STATFJORD FM. deposits. The DUNLIN GP. is mostly deposited in shallow marine and open marine environment with shale, silt and fine sand. The reservoir quality is relatively poor, apart from COOK 2 FM., which contains 20-25 m of good to moderate quality reservoir sands.

The DUNLIN GP. was deposited in the Early Jurassic (190-174 mya) and is dividing the two main reservoirs STATFJORD FM. and BRENT GP. in the Statfjord Field. A paleogeographic reconstruction of the Earth in the Early Jurassic (approx. 200 mya) is shown in Figure 1.4, showing the presence of shallow marine environment in this area during this geological period, consistent with DUNLIN GP. deposits.

**Brent Gp.** The BRENT GP. was deposited during the Mid-Jurassic over a period of roughly 10 million years, and is divided into two main reservoir units, the Lower Brent representing a regressive trend and the Upper Brent representing a transgressive trend. A regional uplift initiated the formation of a deltaic clastic wedge, namely the Brent Delta.

**Lower Brent (LB)** In order moving upwards, Lower Brent consists of BROOM FM., RANNOCH FM and ETIVE FM. The BROOM FM. is a sheet sand, deposited as storm deposits and small distal bars buildups on a shallow marine platform in the Aalenian period (175 mya), and marks the base of the Brent Delta complex. A strong thinning trend is observed S-N, due to regional uplift in the north. A high content of Kaolinite results in a very poor reservoir quality.



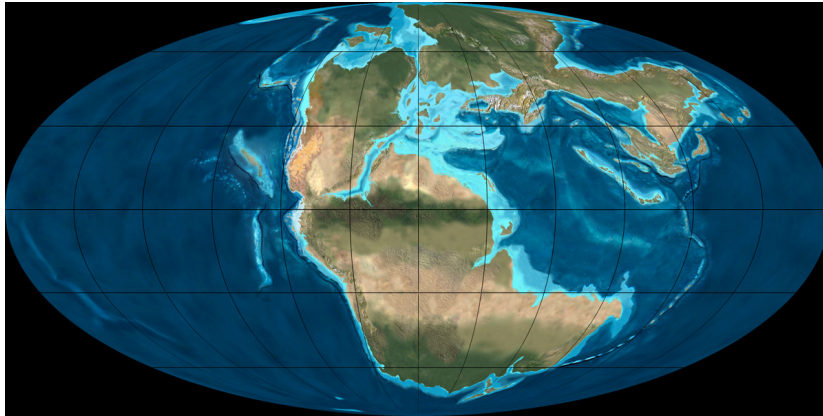


Figure 1.4: Paleogeographic reconstruction of the Earth in the Early Jurassic, 200 mya [1]. Area contemporary known as Norway is located near the lateral center about  $50^{\circ}$  N.

RANNOCH FM. is defined as a prograded, storm dominated delta front. It was deposited as the Brent Delta was prograding outwards into the sea during this regressive period. This trend is reflected in the subdivision of RANNOCH FM. into RANNOCH 1 FM., which represent the distal parts of shore face units, and RANNOCH 2 FM., which represent the lower/middle shore face environment.

ETIVE FM. represents the delta front/upper shore face environment (marginal marine). Together with RANNOCH 2 FM., it possess excellent reservoir quality. ETIVE facies is grading into RANNOCH 2 FM. within cyclic units, and similar grading between RANNOCH 2 FM. and RANNOCH 1 FM is observed.

**Upper Brent (UB)** Upper Brent consists of NESS FM. and TARBERT FM. A 20 m thick claystone in the lowermost part of the NESS FM. called “Mid Ness Shale”, represents a significant pressure barrier and separates Upper from Lower Brent. In the Statfjord Field, the NESS FM. is characterized by highly layered mudrocks, coal and sandstones of coastal plain to shallow marine depositional origin. In the lower part, coastal plain and tidal flat fines and crevasse splays, lagoonal and low energy bay mudstones and tidal and fluvial channel sandstones. Upper part, coarsening up wave dominated bay fills.

The base of the TARBERT FM. is defined by a flooding of the NESS FM. coastal plain and shallow bays. The TARBERT FM. is present with variable thickness and character throughout the Brent depositional province. It is composed mainly of shallow marine sandstones that were deposited as prograding units on top of NESS FM. during the overall retreat of the Brent depositional system.

**Viking GP.** The VIKING GP. consists of HEATHER FM. and DRAUPNE FM. on the MAIN FIELD, and on the EAST FLANK it includes REWORKED BRENT

sediments of late Middle - Upper Jurassic age.

Transgression resulted in a flooding of the Brent Delta, and thus HEATHER FM. is deposited as shallow marine silty claystones with high influx of terrestrial plant debris deposited in Mid Bathonian - Mid Oxfordian (160 mya). An unconformity formed when uplifted during the Late Cimmerian rift phase of late Oxfordian - Mid Kimmeridgian (155 mya), separates HEATHER FM. from DRAUPNE FM.

DRAUPNE FM. is deposited under anoxic marine conditions with black, organic rich claystones, and is considered as the main source for the Statfjord Field.

**Formation of the East Flank** The Late Cimmerian NE-SW extension reactivated faults from Early Cimmerian rifting. During uplifting the foot wall blocks became gravitationally unstable and exposed, and many slump blocks moved down along main detachment zones in shales of MID NESS SHALE, MID DUNLIN GP and LOWER STAFJORD FM. Pressure communication across faults in the EAST FLANK is generally good. The foot wall uplift tilted the MAIN FIELD towards NW, with the important result of creating a structural trap.

**Reworked Brent** REWORKED BRENT was deposited as exposed parts eroded and broken apart while being transported down slope as mudslides/earth flows and are found on top of intact EAST FLANK BRENT or DUNLIN strata. They become thinner and more disaggregated eastwards from the crest. See Figure 1.3.

### 1.2.3 Source rocks and migration paths

Large quantities of organic material, mostly Type I kerogen, was preserved in the anoxic depositional environment of DRAUPNE FM. The supply of dissolved oxygen is insufficient for the oxidation of the organic matter. During the depositional history of the area, the organic rich DRAUPNE FM. was buried at depths putting it in the “oil window”, where the temperature is high enough to convert the kerogen to crude oil, but not too high resulting in over maturation.

Geochemical analysis of the oils in the Statfjord and Brent reservoirs of the Statfjord Field indicate that they are charged from DRAUPNE shales in the Viking Graben and East Shetland basins to the south and the Marulk basin to the north. Modeling demonstrates that oil migrates downwards into adjacent sandstones, and laterally either within the Middle Jurassic BRENT GP. or Upper Jurassic MUNIN FM. sandstones. Thereafter oils moves up dip in a fill-spill chain and may migrate from one reservoir level to another depending upon the juxtapositions of the relative stratigraphic units across faults. Finally accumulating at locations such as the structural trap at the crest of the Statfjord Field. Migration has probably taken place from the Paleocene (65 mya) up to present.

### 1.2.4 Statfjord Late Life (SFL)

Until the start up of SFL in 2007, the main drainage strategy of the Statfjord field has been pressure maintenance by water and gas injection. With this strategy, the field was planned to be shut down by now. However, by implementation of the new strategy with pressure depletion in the SFL project, the lifetime of the field is expected to extend until 2020.

The project gave the basis for three major building blocks [2]:

- A comprehensive well investment program in order to produce with the reduced reservoir pressure.
- Offshore installation modifications both to facilitate low pressure production and to be able to handle the 10 year extended life time of the field.
- A new gas export pipeline to UK FLAGS system to provide additional offtake possibility for the produced gas.

Changing the drainage strategy from pressure maintenance to pressure depletion requires an extensive reduction of the reservoir pressure in both the BRENT GP. and the STATFJORD FM. Water and gas injection was stopped, and the pressure is now below the bubble point in the BRENT GP. The liberated gas is not yet mobile, and the “gas bubble” expected in the production facilities is imminent. The expected development of fluid flow in the reservoir during the SFL is illustrated in Figures 1.5 and 1.6.

As Figures 1.5 and 1.6 show, the expected effect of the depressurization results in a reservoir pressure below the bubble point of the oil, and dissolved gas will be liberated. The gas will then migrate towards the crest, from where it will be produced. Some free gas is initially present in the STATFJORD FM. as a result of the earlier upflank gas injection.

Based on technical studies and experience from the Brent field in the UK, uncertainty associated with a depressurization project is represented by the multiphase flow parameters. For the Statfjord field, the following critical issues and parameters were identified [2]:

- Critical gas saturation ( $S_{gr}$ )
- Relative gas permeability ( $k_{rg}$ )
- Relative oil permeability to gas ( $k_{rog}$ )
- Residual oil saturation after gas flood ( $S_{ogr}$ )
- Scaling up multiphase flow parameters to a full field model scale

This thesis mainly considers the 1<sup>st</sup>, 2<sup>nd</sup> and 5<sup>th</sup> point in this list, the upscaling of relative gas permeability and critical gas saturation.

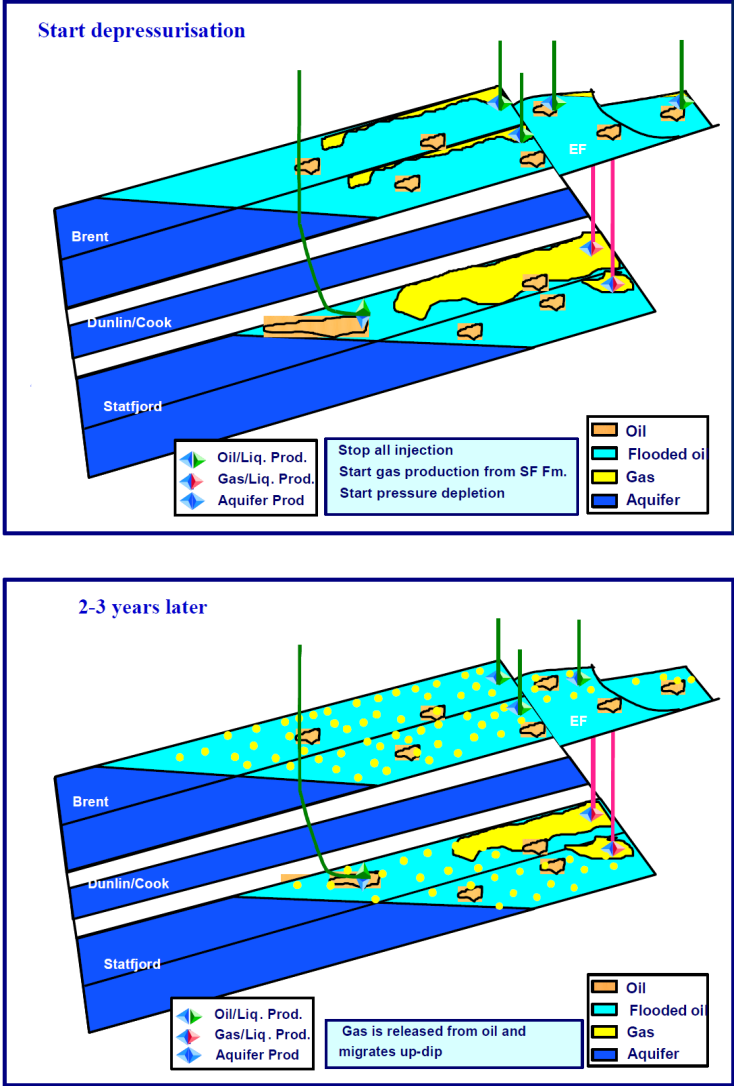


Figure 1.5: Illustration of the SFLL depressurization process [2].  
(Continues in Figure 1.6)

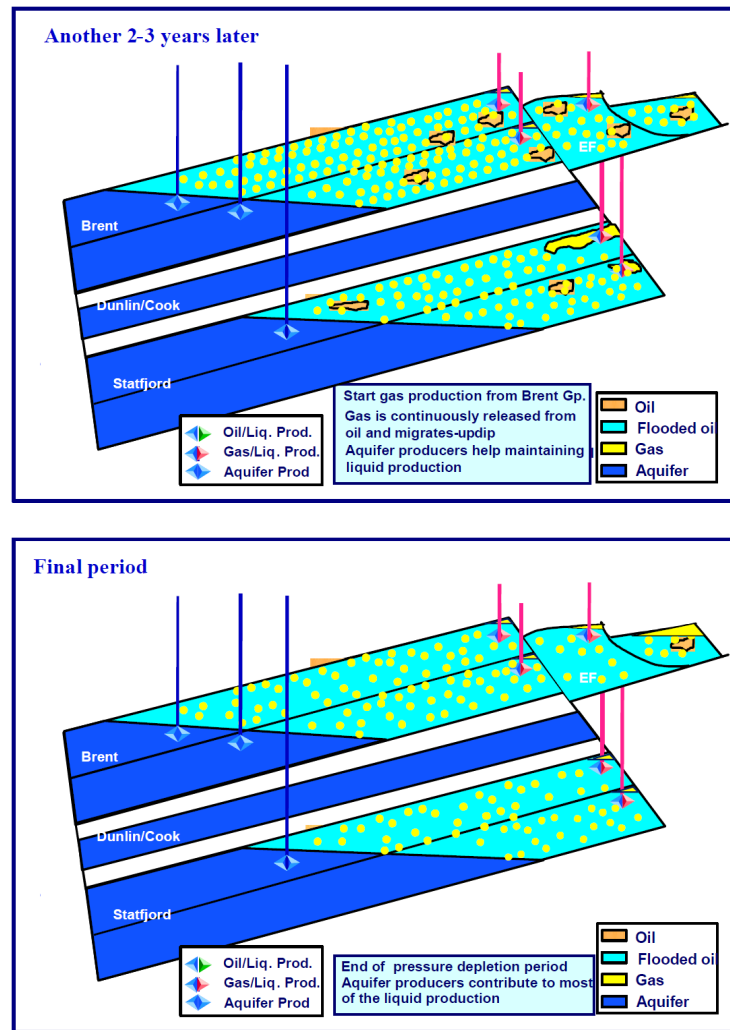


Figure 1.6: Illustration of the SFLL depressurization process [2].  
(Continuation of Figure 1.5)

### 1.3 Reservoir simulation

*Reservoir simulation* is a numerical approach to define and calculate flow patterns in a reservoir by use of models. Due to the approach, reservoir models are often referred to as *numerical models*. Based on fluid flow equations on differential form and basic mass conservation principle, the mathematical problem defined by a model becomes very complex. In order to simplify the problem, numerical techniques are required to solve it. Hence, analytical (exact) solutions are not the objective of simulations. However, input of correct and sufficient data will give a good approximation. The software used to perform the numerical calculations is referred to as a *reservoir simulator*. The reservoir simulator requires access to a powerful CPU in order to perform the large amount of computations the process generates. Most of the theory described in this subsection is gathered from [5].

#### 1.3.1 Reservoir simulation study

Planning and carrying out a reservoir simulation study follows a general procedure [10]:

**Problem Definition** Definition of the problem must clearly state the practical objective of the study and which factors are dominating, and sufficient information about the reservoir must be gathered. When defining the problem, proper planning is essential to ensure good and proper use of resources (i.e. right people and information at the right time).

**Data Acquisition and Review** Data collected has to be reviewed, quality controlled and organized in order to avoid both unnecessary workloads and errors supplied to the model. A simulation model requires large amounts of input data. Type of input data depends on several factors defined in the study. The composition of each phase is crucial to establish if a *compositional model* is chosen, and will be of little importance if a *black oil model* is considered. On the other hand, the type of data needed can differ as a result of defining the objective of a study. If the simulation aims to evaluate the regional pressure communication in an entire field, the input data required and critical factors will be very different from a case where the aim is to evaluate well targets by simulating more local behavior.

**Reservoir Description and Model Design** The description of the reservoir and the fluids involved influence the type of model chosen to simulate the problem. Choosing the right design involves type of process to be modeled, problems related to fluid mechanics, the objective of the study and data quality.

**History Matching** When building the model, the reservoir has in some cases already been produced for some time. Running the model to compare results with the actual producing history is an important part of adapting the model.

If there is a large difference between simulated and actual behavior, the input data of the model should be evaluated and adapted until an acceptable history match is obtained. History matching should be an ongoing process throughout the production period of a reservoir to maintain an “updated” model to be able to predict future behavior.

**Predictions** History matching makes a model more reliable for predictions, which often is the main objective of a reservoir simulation study. A good model used for predictions helps engineers make the “right” decisions. Reservoir development and production strategy is based on expected behavior of a reservoir, hence predictions combined with experience constitute the basis for great economical decisions.

**Report** The results and conclusions are summarized in a final report.

### 1.3.2 Black Oil Model

As mentioned in 1.3.1, the model design that best describes the problem defined has to be chosen. In the Statfjord Field, and in this thesis, the model of choice is the frequently used *Black Oil Model*. It is based on treating only two hydrocarbon components, oil and gas, in addition to water component. This implies that change of composition of the hydrocarbon components are not considered, hence fluid properties can be treated as functions of pressure and solution gas-oil ratio. The contrast would be *Compositional Model*, where each hydrocarbon component (i.e.  $C_1$ ,  $C_2$ ,  $C_3$ ... etc.) is treated separately, allowing change of composition of both the oil and the gas. The basic assumptions for a *Black Oil Model* are:

- Three *phases*; oil, gas and water
- Three *components*; oil, gas and water (“components” refers to the distinct fluids at a reference state, normally standard conditions)
- No phase transfer between water and hydrocarbons
- A part of the gas component can be dissolved in oil and flows together with the oil component in an oil phase
- All of the oil component is in oil phase
- Constant temperature

To adapt the *Black Oil Model* to fit the Brent reservoir in the Statfjord Field, an additional assumption is made to modify it:

- Oil component can be dissolved in the gas phase

The *Black Oil Model* with this additional assumption is actually referred to as a *Gas Condensate Model*.

### 1.3.3 Input Data

Reservoirs are not homogeneous, and properties of the reservoir will vary depending on location. Permeability and porosity are examples of such properties. Due to this variation, it is practical to divide the reservoir into smaller regions with its belonging properties in the model. The result of this division is a *grid*, where each cell/piece is called a *grid block*.

**Grid** Defining a grid can be challenging when the reservoir is very complex. The knowledge of reservoir geometry is normally based on interpretation of seismic data in correlation with well data. Reservoir properties are also estimated based on seismic interpretation and well data, with the addition of a geological understanding of depositional environments. However, reservoir properties can only be measured in the wellbore, and any property assigned between two wells is of great uncertainty and subject to continuously improvement.

The grid in a geological model is often of high resolution. The high resolution grid includes local variations in different properties like channel sands and local flow barriers. The computational time of a reservoir simulation is proportional with the number of grid blocks. In order to create a grid which is applicable and efficient, an upscaling procedure is required. The grid from a geostatistical realization is upscaled to a coarse grid model where properties for new grid blocks are calculated as an average value of the parent grid blocks. Different methods are used for the averaging. However, all methods of averaging aims to preserve critical factors influencing flow patterns. An excessive upscaling by unifying too many grid blocks from the geostatistical model would make the model too inaccurate. This taken into consideration, a compromise must be found between preserving the small variations and keeping the data quantities time efficient when creating the grid (example shown in Figure 1.7).

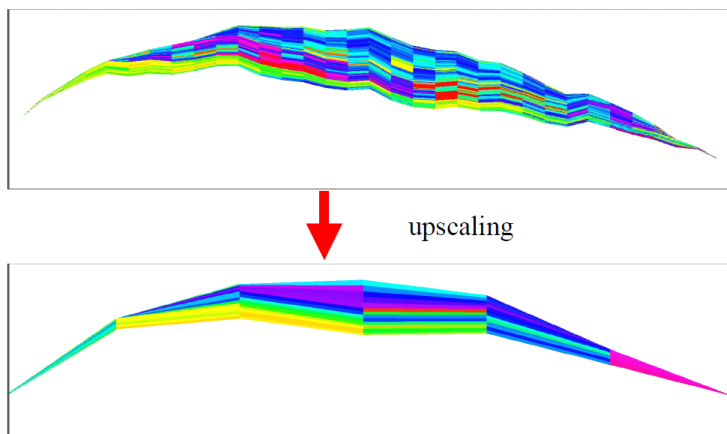


Figure 1.7: Upscaling from geostatistical realization to simulation grid, cross section view [5].



A grid is needed for numerical computations. The solution is represented as average computed values for each grid block. As a result of pressure difference between the blocks, flow is modeled taking place across the boundary between them.

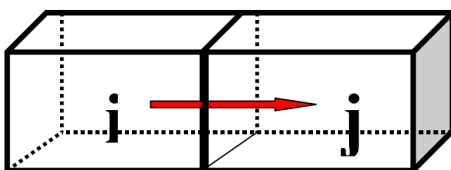


Figure 1.8: Flow between grid blocks  $i$  and  $j$  [5].

The flow between grid blocks  $i$  and  $j$  shown in Figure 1.8 is computed using Darcy's Law:

$$q_l = \frac{A k k_{r,l} \rho_l}{\mu_l} \frac{p_j - p_i}{\Delta x_{ij}}, \quad (1.1)$$

where  $l$  denotes the phase,  $q$  is flow rate,  $A$  is cross sectional area on the boundary,  $k$  and  $k_{r,l}$  are absolute and relative permeability,  $\rho$  is density,  $\mu$  is viscosity,  $\Delta x_{ij}$  is the distance between block centers and  $(p_j - p_i)$  is the pressure difference, and flow is caused by non zero pressure gradient. Pressures and saturations at initial equilibrium can be calculated with a minimal amount of input data. The non zero pressure gradient is obtained from initial equilibrium when adding a source/sink term to Darcy's Law combined with mass conservation.

**Rock properties** *Absolute permeability* ( $k$ ) and *porosity* ( $\varphi$ ) are assigned to each grid block. Absolute permeability is dependent on direction and independent of pressure, while porosity is dependent on pressure and accounted for by introducing *rock compressibility* ( $c_r$ ). Absolute permeability and porosity are obtained from core analysis, logging, well testing and seismic interpretation. Distribution is computed in a fine scale geostatistical realization, and an up-scaling procedure as mentioned in the grid section is required to import these parameters into a coarse simulation grid.

**Fluid Data** Fluid properties must be supplied to a simulator in addition to reservoir description given by absolute permeability and porosity. The amount of input data needed for fluid property calculations depends on the type of model to be used. This thesis considers the *Black Oil Model* with the addition of oil components can be dissolved in the gas phase. Volume factors ( $B_l$ ) is defined as the volume of a certain amount of a phase at reservoir conditions divided by the volume this amount occupies as the same phase at surface conditions. The surface conditions is a reference state often referred to as *standard conditions*. Volume factors are functions of reference state and pressure. Viscosities ( $\mu_l$ ) of the different phases are also needed. In addition one needs to quantify mass transfer between oil and gas by introducing gas/oil ( $R_s$ ) and oil/gas ( $R_v$ ) ratio.

**Saturation Functions** In order to solve the numerical model, a set of *saturation functions* need to be defined. Saturation functions describe the flow behavior depending on the saturation ( $S_l$ ) of the respective phase considered. One of these saturation functions is the *relative permeability* ( $k_{rl}$ ) ( $l$  denotes the type of phase, i.e. oil, gas or water in this thesis).

**Relative permeability** If several phases are flowing simultaneously, the effective (*relative*) permeability of each phase depends on the saturation. This saturation function will be described in greater detail, since it is the subject of investigation in this thesis. The relative permeability is the fraction of the absolute permeability available for flow of phase  $l$ , and is defined as

$$k_{rl} = \frac{k_l}{k}, \quad (1.2)$$

where  $k_l$  is the phase permeability available and  $k$  is the absolute permeability. Relative permeability is dimensionless and a number between 0 and 1 ( $k_l \leq k$ ). Experimentally, the work on relative permeabilities is mostly performed on two-phase systems of oil/water or oil/gas. The relative permeability of water ( $k_{rw}$ ) and oil ( $k_{row}$ ) in an oil/water system are measured as functions of water saturation ( $S_w$ ). Similarly, the relative permeability of gas ( $k_{rg}$ ) and oil ( $k_{rog}$ ) are measured in an oil/gas system as a function of gas saturation ( $S_g$ ). Figure 1.9 shows a typical result of measurements of relative permeabilities in two-phase systems.

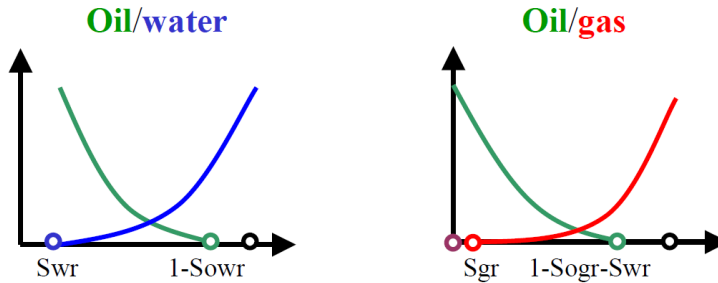


Figure 1.9: Two-phase relative permeability data [5].

The endpoint saturations of oil ( $S_{owr}$  in a oil/water system,  $S_{ogr}$  in a oil/gas system), water ( $S_{wr}$ ) and gas ( $S_{gr}$ ) are all of great importance for initial distribution and final recovery, and is reflected by the largest saturation of a phase for which the relative permeability of the respective phase in the respective system is zero. Relative permeability is imported to the model as four different tables reflecting the four measured two-phase curves  $k_{rw}$ ,  $k_{row}$ ,  $k_{rg}$  and  $k_{rog}$ . If all three phases are flowing simultaneously, three-phase relative permeability must be constructed from the four tables obtained from the measurements. This is usually done by considering the following:

- The curve  $k_{rw}$  obtained from the two-phase oil/water system as a function of  $S_w$  is used as water relative permeability.
- The curve  $k_{rg}$  obtained from the two-phase oil/gas system as a function of  $S_g$  is used as gas relative permeability.
- Relative permeability of oil ( $k_{ro}$ ) in the three-phase system is a function of both  $S_w$  and  $S_g$  (i.e.  $k_{row}$  and  $k_{rog}$  from the two-phase systems), and has to be constructed. An averaging with saturations as weighting functions gives BAKER'S FORMULA

$$k_{ro} = \frac{S_g k_{rog} + (S_w - S_{wr}) k_{row}}{S_g + S_w - S_{wr}}. \quad (1.3)$$

Alternatively, STONE'S SECOND FORMULA

$$k_{ro} = k_{row}^* \left[ \left( \frac{k_{row}}{k_{row}^*} + k_{rw} \right) \cdot \left( \frac{k_{rog}}{k_{row}^*} + k_{rg} \right) - (k_{rw} + k_{rg}) \right], \quad (1.4)$$

where  $k_{row}^* = k_{row}(S_{wr})$ , can be used.

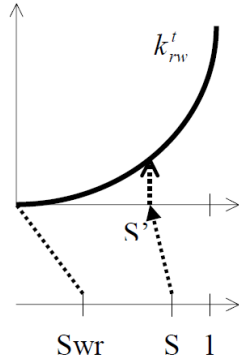
**End point relative permeability scaling** Relative permeability curves can be different depending on location in the grid, represented by a different function shape, mobile saturation interval or in function value by a multiplication factor. Hence, more than one set of saturation function tables is needed. The reservoir can be divided into a small number of flow units with belonging saturation tables. Nevertheless, modification on grid block level can be done by using a saturation scaling procedure. Saturation end points available for change are:

- $S_{wr}$  (critical water saturation)
- $S_{gr}$  (critical gas saturation)
- $S_{owr}$  (critical oil saturation for oil/water system)
- $S_{ogr}$  (critical oil saturation for oil/gas system)

Modification of saturation function values are obtained by defining:

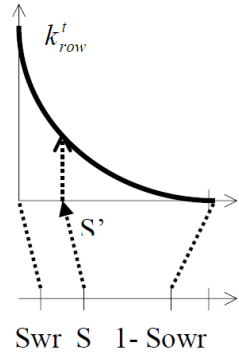
- $KRW$  (maximum water relative permeability,  $k_{rw}(1)$ )
- $KRG$  (maximum gas relative permeability,  $k_{rg}(1 - S_{wr})$ )
- $KRO$  (maximum oil relative permeability in any oil table,  $k_{row}(S_{wr})$  and  $k_{rog}(0)$ )

If normalized saturation functions  $k_{rw}^t$ ,  $k_{row}^t$ ,  $k_{rg}^t$  and  $k_{rog}^t$  are input values to the model, specified end point values  $S_{wr}$ ,  $S_{gr}$ ,  $S_{owr}$ ,  $S_{ogr}$ ,  $KRW$ ,  $KRG$  and  $KRO$  in a grid block gives relative permeabilities as follows in Figure 1.10.



$$S' = \frac{S - Swr}{1 - Swr}$$

$$k_{rw}(S) = KRW * k_{rw}^t(S')$$



$$S' = \frac{S - Swr}{1 - Swr - S_{owr}}$$

$$k_{row}(S) = KRO * k_{row}^t(S')$$

Figure 1.10: Calculation of relative permeabilities from normalized saturation functions and end point values, where  $S'$  is the normalized water saturation [5]. The calculations to obtain  $k_{rg}$  and  $k_{rog}$  from  $k_{rg}^t$  and  $k_{rog}^t$  are similar.

**THE COREY CORRELATION** is another method for creating relative permeability curves. The correlation uses normalized saturation as input,  $S'$  (in oil/water system, the normalized water saturation is used. In oil/gas system, the normalized gas saturation is used), and the COREY EXPONENT for each phase,  $N_{w,o,g}$ . Considering relative gas permeability, the COREY CORRELATION becomes

$$k_{rg}^t(S'_g) = (S'_g)^{N_g} \tag{1.5}$$

The denormalized curves are then given by

$$k_{rg}(S_g) = KRG \cdot (S'_g)^{N_g} = KRG \cdot \left( \frac{S_g - S_{gr}}{1 - S_{wr} - S_{gr}} \right)^{N_g} \tag{1.6}$$

Relative permeability for water and oil is calculated the same way. However, the normalized oil saturation is expressed by normalized water saturation in oil/water systems ( $1 - S'_w$ ), and by normalized gas saturation in oil/gas systems ( $1 - S'_g$ ).

**Capillary pressures** A second set of saturation dependent parameters is capillary pressures ( $P_c$ ), and describes the relation between phase pressures. It is defined as the pressure difference between 2 phases:

$$\text{oil/water} : P_{cow} = p_o - p_w \quad (1.7)$$

$$\text{gas/oil} : P_{cgo} = p_g - p_o, \quad (1.8)$$

where  $p$  is the phase pressure of water, oil or gas denoted by  $w$ ,  $o$  and  $g$  respectively.  $P_{cow}$  is the capillary pressure between oil and water, and assumed a function of  $S_w$ .  $P_{cgo}$  is the capillary pressure between gas and oil, and assumed a function of  $S_g$ . These relations are needed together with mass balances to determine unique solutions of reservoir fluid flows, and are important to determine the initial distribution of the phases in a reservoir.

### 1.3.4 Reservoir Simulator

A computer program supplied with sufficient input data from the model is needed to calculate the reservoir fluid flow. Mass balance equations on differential form is solved by approximating them as differences followed by a linearization process. Together with supplied boundary conditions and elimination with use of capillary pressure relations, the linear equations is solved. A commonly used reservoir simulation program is ECLIPSE™. Originally developed by ECL (Exploration Consultants Limited), it is owned , developed, marketed and maintained by a division of SCHLUMBERGER called SIS [16]. The program runs by calling an input *data file* and it comes in two main versions:

- ECLIPSE100 solves the black oil equations on corner-point grids
- ECLIPSE300 solves compositional and thermal processes

The structure of the data file called by ECLIPSE, must be programmed with several main sections appearing in a specific order, though some sections are optional. The order of the sections are as follows (the sections are required unless otherwise noted) [11]:

RUNSPEC	contains the title together with option switches and declaration of problem dimensions like wells, grid size, phases present, start date etc.
GRID	Specification of the geometry of the computational grid, including rock properties like porosity, absolute permeability and net-to-gross assigned to each grid block.
EDIT	( <i>optional</i> ) This section includes the option of entering modifications to calculate pore volumes, grid block center depths and transmissibilities.

## 1 INTRODUCTION

---

- PROPS** All pressure and saturation dependent functions are to be included in this section. This includes density, viscosity, relative permeability and capillary pressure. If the model is compositional, it also includes the equation of state (EOS) description.
- REGIONS** (*optional*) If grid regions are required, this section govern the division of the grid into sections/regions for calculation of PVT properties like densities and viscosities, saturation properties like relative permeabilities and capillary pressures, initial conditions, fluids in place and EOS regions. If this section is not included, only one region exists and constitute the entire grid.
- SOLUTION** The initial conditions in the reservoir is specified in this section. Initial conditions can be calculated using specified fluid contact depths to give potential equilibrium, read from a restart file set up by an earlier run or specified by the user for every grid block.
- SUMMARY** (*optional*) If data are to be written to a SUMMARY FILE for graphical or computational review at specified time steps, it must be declared in this section.
- SCHEDULE** In this section production/injection controls and constraints are specified together with times at which output reports are created. In addition, it is possible to specify vertical flow performance and simulator tuning parameters.
- OPTIMIZE** (*optional, ECLIPSE 300 only*) Specifies a reservoir optimization problem with objective function, control parameters and constraints.

The structure within each section in the data file is somewhat optional and commands is governed by a keyword system. Prepared as free format, any standard editor may be used to prepare the input data file [12]. The use of the abundant number of keywords is described in detail in [11], and is of great help and support when writing a data input file.

### 1.3.5 Post processing software

- S3GRAF** is a program which can read the output files from the simulation done with ECLIPSE and create plots for comparison of results. It also provides a 3D visualization with very similar functions as FLOVIZ described below.
- FLOVIZ** gives the opportunity of a 3D visualization of the reservoir with its grid blocks, properties and well locations. The program comes with the ECLIPSE program package, and is therefore well suited for reading ECLIPSE output files. Properties are displayed by assigning colors to different values, presenting the property as a color scale and filling each cell with the belonging color. Time dependent properties

can be displayed at a single time step, or played in a sequence as an animated property development through time.

RESVIEW is a UNIX based 3D visualization program [13], with similar possibilities as in FLOVIZ. However, RESVIEW is more advanced and gives more opportunities to modify the grid and export the modified parameters as an ECLIPSE input file. One of the advantages is the possibility of programming files, called *batch files*, to perform numerous operations in RESVIEW in a specified order.

## 1.4 Upscaling

Considering a coarse grid block containing a relatively small amount of gas. If a vertical flow barrier exists on top of the coarse grid block, low horizontal fluid velocity will allow gas to segregate to the top part of the block, and form a thin layer of gas with high mobility. The average gas saturation of the block will still be very small, however the gas will be produced with higher rates than with evenly distributed gas saturation in the grid block. Using the critical gas saturation and relative permeability curves from core analysis will not allow this thin layer of gas in a coarse block to flow when simulating. The situation is visualized in Figure 1.11. When upscaling, this effect must be included. A method for this upscaling is proposed in this section.

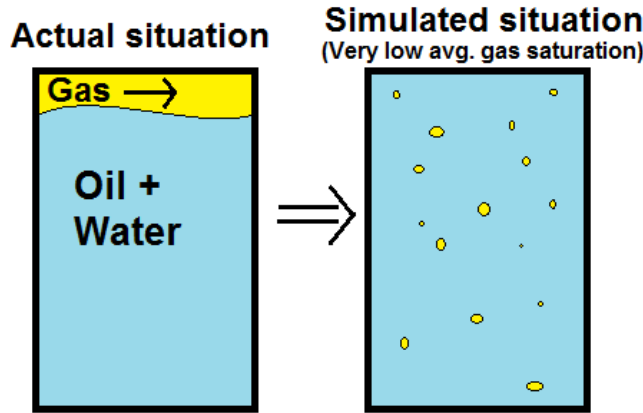


Figure 1.11: A visualization of the difference between simulated and “real” situation, when a thin layer of gas flows with high mobility in a coarse grid block.

The discretized flow equations for the *Black Oil Model* contains a well known term, called the *Transmissibility* given by

$$T_x = \frac{k_x \cdot A}{\Delta x}, \quad (1.9)$$

where  $x$  denotes the direction of flow,  $T$  is the transmissibility,  $k_x$  is the absolute permeability (which is assumed to be a diagonal tensor),  $A$  is the cross sectional area on the boundary through which the flow occurs and  $\Delta x$  is the distance between block centers.

When upscaling relative permeability, it has been pointed out that a Transmissibility weighted upscaled relative permeability should be used [17]. Considering the upscaling of the blocks drawn with thin lines in Figure 1.12, the Transmissibility weighted upscaled relative permeability can be calculated using

$$k_{rg}^{avg} = \frac{\sum_{i=1}^5 k_{rg,i} \cdot T_i}{\sum_{i=1}^5 T_i}, \quad (1.10)$$



where  $k_{rg}^{avg}$  is the upscaled relative gas permeability,  $k_{rg,i}$  is the relative gas permeability of cell in layer  $i$ , and  $T_i$  is given by Equation 1.9 for the cell in layer  $i$ .

In this thesis, the values will be written from a fine grid model when simulated with ECLIPSE. Equation 1.10 will then be calculated using

$$k_{rg}^{avg} = \frac{\sum_{i=1}^n k_{rg,i} \cdot k_{x,i} \cdot \Delta y_i \cdot \Delta z_i \cdot NTG_i}{\sum_{i=1}^n k_{x,i} \cdot \Delta y_i \cdot \Delta z_i \cdot NTG_i}, \quad (1.11)$$

where  $i$  denotes the layer number,  $\Delta y_i \cdot \Delta z_i$  is the cross sectional area on the boundary of the cell in layer  $i$  through which the flow occurs,  $NTG_i$  is the net-to-gross ratio of the cell in the layer,  $k_{x,i}$  is the absolute permeability in X-direction and  $k_{rg,i}$  is the relative gas permeability of the cell. An assumption is made in Equation 1.11. The distance between block centers,  $\Delta x$ , is left out since the refined grid model will differ very little in this value within the cells/layers the upscaled relative permeability is calculated for. The value would be canceled out in the weighting. The distance between block centers should be evaluated if block geometry differs greatly.

An alternative method for calculating the transmissibility weighted relative permeability would be to write the value of transmissibility directly from simulation using ECLIPSE, and apply this value using Equation 1.11. This will include difference in both dip and distance between cell centers. In this thesis, the upscaling will be done by evaluating the values in Equation 1.11, and is assumed to be adequate.

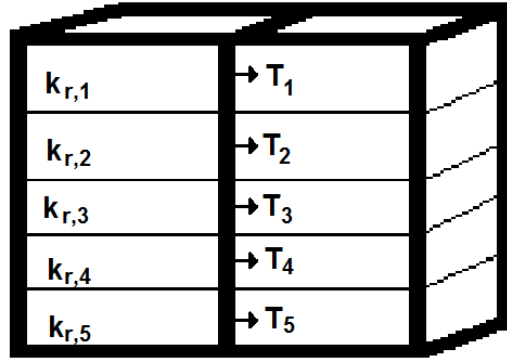


Figure 1.12: Transmissibility at the interface between two adjacent coarse blocks. Blocks drawn with thin lines is upscaled into blocks drawn with thick lines.

The average saturation for the coarse block is calculated using a pore volume weighted approach.

$$S_g^{avg} = \frac{\sum_{i=1}^n S_{g,i} \cdot PV_i}{\sum_{i=1}^n PV_i}, \quad (1.12)$$

## 1 INTRODUCTION

---

where  $S_g^{avg}$  is the average gas saturation,  $S_{g,i}$  is the gas saturation in the cell in layer  $i$  and  $PV_i$  is the pore volume of the cell.

Relative permeability curves are created from the transmissibility weighted average relative permeability and the pore volume weighted average saturation. The two values are plotted against each other for each coarse grid block in the layer upscaled at every time step. It will differ between cells in X-direction evaluated. A best match curve is created using the least square method and assuming a normalized Corey relative permeability curve,

$$SQ_i = \left( \frac{k_{rg,i}^{corey} - k_{rg,i}^{avg}}{k_{rg,i}^{avg}} \right)^2, \quad (1.13)$$

where  $i$  denotes the time step,  $SQ_i$  is the square at time step  $i$ ,  $k_{rg,i}^{avg}$  is calculated using Equation 1.11 with measured values at time step  $i$  and  $k_{rg,i}^{corey}$  is the relative gas permeability calculated from the assumed normalized Corey relative permeability curve. However, the Corey relative permeability is denormalized using  $S_{gr}$  and  $S_{wr}$  to be able to match it with  $k_{rg,i}^{avg}$  (see Equation 1.6). Solving

$$\sum_{i=1}^n SQ_i = \min \quad (1.14)$$

by varying the Corey exponent,  $N_g$ , and the critical gas saturation,  $S_{gr}$ , for the assumed normalized Corey curve, will give an input normalized relative permeability curve for ECLIPSE to apply to the upscaled layer.

This yields a modification of the critical gas saturation and saturation number for the layer upscaled, when simulating the upscaled model with ECLIPSE.

## 2 Building an applicable model

The scope of this thesis is to study the effect of gas becoming mobile within thin layers with high relative gas permeability in the Statfjord field, and how to model this in a coarse grid simulation model to include the effect. An applicable model is needed. The model has to represent the Statfjord field reservoir structure and model fluid flow during the expected pressure development. It must reflect the complexity of the structure and fluid flow in the field. However, it must have a run time which allows use of the model to evaluate different scenarios.

### 2.1 Grid and input parameters exported from FFM2005

To create the model used for this study, a WNW-ESE cross section of the STATFJORD FULL FIELD MODEL (FFM2005) is chosen, such that it is representative for the general understanding of the structure and fluid flow of the actual reservoir. By only evaluating this 2D slice, the model is simple and manageable. This simplification can cause the loss of complex fluid flow patterns and effects from the 3D model, and makes the 2D slice model not directly representative. However, it is reasonable to assume that the obtained trends in the upscaling from the 2D slice will be applicable in 3D upscaling. Since the field consists of two horizontally separated main reservoirs and the biggest effect of SFLL is expected in the upper reservoir, only the model for the BRENT GP. has been used.

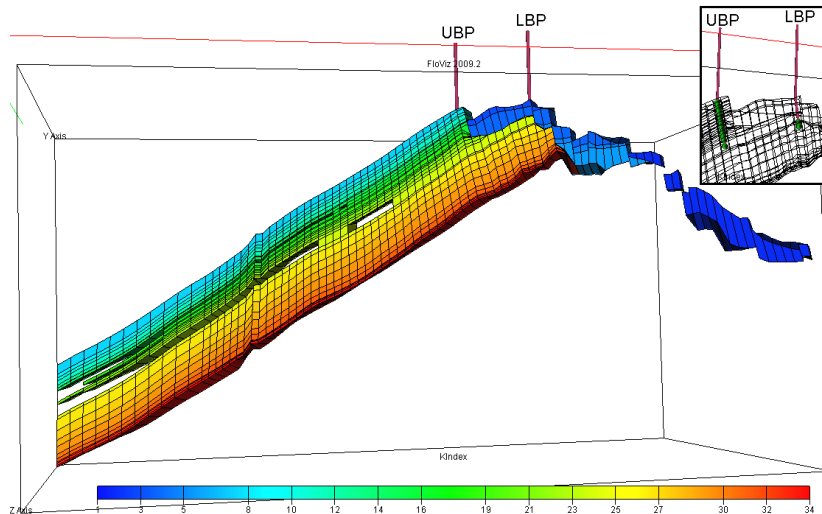


Figure 2.1: Visualization of the grid for the basic model first created to represent the BRENT GP. of the Statfjord field. Color scale represents the index of the layers. A visualization of the perforations is included in the top right box.

The grid of FFM2005 - BRENT GP. (dimensions:  $111 \times 114 \times 34 - \vec{i}, \vec{j}, \vec{k}$ )

is imported to RESVIEW together with initial parameters and restart parameters from the history matching (February 1 - 2007). Even though the FFM2005 is history matched up to date, the restart parameters are chosen at February 1 - 2007. This choice is due to the fact that the effect of pressure depletion is expected to occur some time after 2007. To be sure to evaluate the full effect of gas liberated from the oil, the model is restarted at a point prior to this effect of pressure depletion. A layer overview shown in Figure A.2 on page 76 gives the relation between geological layers and the representative sections in the reservoir model. Using RESVIEW, the cross section 1-111  $\vec{i}$ , 43-43  $\vec{j}$ , 1-34  $\vec{k}$  from the original grid is chosen. All cells not included in this slice is deleted, giving the new grid dimensions 111x1x34 -  $\vec{i}$ ,  $\vec{j}$ ,  $\vec{k}$  (see Figure 2.1). The belonging initial and restart parameters are kept for the slice, and exported from ResView as input files for ECLIPSE. The files contain the ECLIPSE keyword for a given parameter and a matrix assigning the respective value to each cell in the grid. An overview of parameters exported from RESVIEW is presented in Table A.1 on page 79. Some input parameters must still be edited or created to be able to run the 2D slice model in ECLIPSE.

Rock and fluid properties from the FFM2005 can be included directly, since they do not depend on the geometry of the grid (e.g PVT-data, rock properties, density and relative permeability curves).

### 2.2 Preparing the model for ECLIPSE

To keep the separated regions from FFM2005 available, the keyword FLUXNUM and belonging input parameters must be created. This is simply done by copying the parameter from the keyword SATNUM for each cell in the model.

The critical gas saturation (keyword SGCR) in FFM2005 has previously been upscaled in some regions to include the effect of reduced critical gas saturation due to gas injection. The initial critical gas saturation in the Statfjord Field is evaluated to be 6,2 %. However, in regions where WAG injection has been carried out, critical gas saturation is recommended set to 5 % [8]. In order to avoid upscaling of a parameter already upscaled, the parameter for all active cells given in the keyword SGCR is set to 6,2 %.

Due to the WAG injection effect, the relative gas permeability (keyword SGFN) curve in some regions has also previously been altered as an upscaling. Initial curves for relative gas permeability with a Corey exponent of 2,5 for all regions are therefore created and used for the 2D slice model in this thesis.

Restart value of the gas saturation is mostly close to zero in the reservoir. In some cells which has a value very close to zero, the exported value from RESVIEW is given as a very small negative integer. This is due to approximations done by RESVIEW when calculating gas saturation from water and oil saturations from restart file. Since negative values of gas saturation is unphysical and ECLIPSE can not interpret negative values, editing of the exported file of the keyword SGAS is needed. All negative values are altered to positive integers (the negative value is very small, magnitude  $10^{-12}$ - $10^{-13}$ , and do not affect

the simulation by only removing the minus sign. This procedure is less time consuming than finding each negative value in the matrix and replacing it with the value zero).

A schedule file is created for ECLIPSE to be able to produce from the reservoir, and is explained in greater detail in subsection 2.3.

A \*.DATA file with all the sections described in sub subsection 1.3.4 on page 19 is needed for ECLIPSE to run the simulation. The file is created in such a way that it contains almost only the command “INCLUDE”, and calls the different files created for input. Other keywords which governs the method of solution ECLIPSE uses, are written in the \*.DATA file (example given in Appendix B on page 83). This structure makes it more efficient to alter the different parameters if needed.

### 2.3 Adapting pressure development

The simplified model is now described by the grid, fluid data and restart parameters (pressures and saturations) obtained from FFM2005. An ECLIPSE \*.DATA file has been created, including the simplified model and using saturation functions from FFM2005. Input data now needed to run a simulation is well specifications in the schedule file. It is chosen to include two producers in the model. “UBP” (Upper Brent Producer) is perforated in all layers above the Mid Ness Shale pressure barrier, in cells  $47 \vec{i}$ , located in the top of the structure. “LBP” (Lower Brent Producer) is perforated in 2 layers below the Mid Ness Shale pressure barrier, in cells  $56 \vec{i}$ , which also are located in the top of the structure (See Figure 2.1). The perforated cells will have different values of  $\vec{k}$  in the different refinements, and must be modified in each case to make sure the same area is perforated.

To obtain the expected pressure development in the reservoir, the model is adapted by controlling and modifying the reservoir volume rate from both producers. Wells will not be controlled by reservoir volume rates in “real life”. However, by controlling the production rates with reservoir volume rates, the pressure development in the reservoir is expected to be the same in all simulations followed in this thesis. The liberation of gas in the reservoir strongly depends on the pressure development, and the reservoir volume rate is chosen as the control mode in order to make the simulations comparable. The two producers, UBP and LBP, is set to produce with similar reservoir volume rates. The rates are found by trial and error until a match is found. The pressure development obtained in the latest prediction run of FFM2005 (February 15 - 2011), called AMAP2011, is plotted and compared with the pressure development in the constructed model of this thesis. This comparison is shown in Figure 2.2, showing a good compliance in the period from Feb-2007 until Jan-2025.

## 2 BUILDING AN APPLICABLE MODEL

---

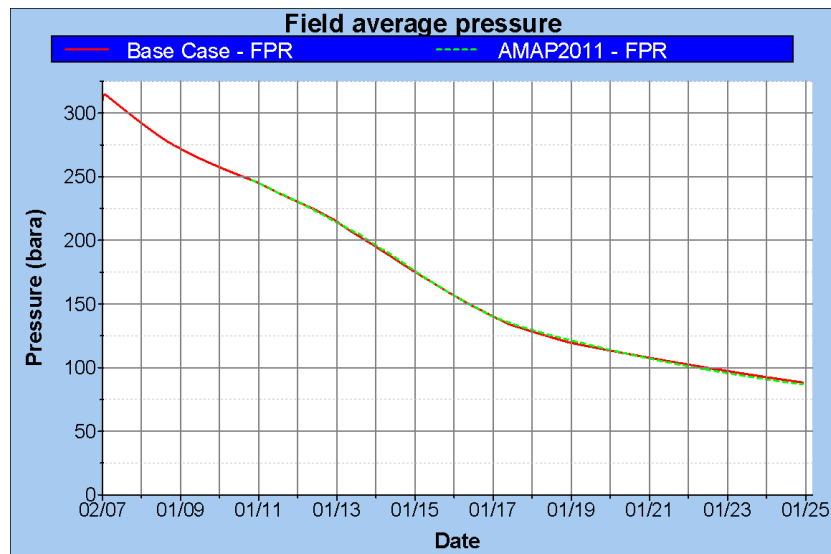


Figure 2.2: Y-axis represents pressure and x-axis represent time. “FPR” is the average field pressure, and the plot compares the expected pressure development from the prediction run AMAP2011 (red) with the pressure development in the constructed model shown in Figure 2.1 (green) in the period February 2007 - January 2025.

### 3 BASE CASE

The pressure development in the 2D simulation model is now consistent with the expected pressure development in FFM2005. In addition, rock properties and fluid properties are adopted from FFM2005 into the 2D simulation model. Using the restart and initial cell values from FFM2005, it is reasonable to expect the behavior of the 2D simulation model to be somewhat similar to FFM2005. The focus is now shifted towards the behavior of the released gas. The initial setting of the 2D simulation model with the two producers, UBP (Upper Brent Producer) and LBP (Lower Brent Producer), will from this point on be referred to as the BASE CASE.

#### 3.1 Focus of comparison

The BASE CASE run will be, as the name suggests, the basis for all analysis and comparison. To study the behavior of the released gas, it has to be decided how to compare models and which parameters to be investigated. When upscaling the relative gas permeability, the result of the upscaling must have a scope or desired parameter to match with the BASE CASE. In this thesis the results desired to focus on is the gas production from the reservoir. Where is the gas produced from, how fast is the gas produced and how does the gas saturation develop in the reservoir when released.

#### 3.2 Simulation results

The BASE CASE is simulated with ECLIPSE, and a visualization of the run is evaluated with FLOVIZ. Gas saturation in the reservoir is low the first few years. However, gas starts to liberate as the pressure drops in the reservoir, and a “gas bubble” is observed in the data. To illustrate this “gas bubble”, a plot using S3GRAF showing *field gas production rate* (FGPR) through *time* is presented in Figure 3.1. The term *field production* will in this thesis be defined by total production from both UBP and LBP. Production of liberated gas is simulated to begin around year 2013-2014 with gas production rates of 20,000-30,000 Sm<sup>3</sup>/d. The rate increases until 2017 with observed rates about 86,000 Sm<sup>3</sup>/d, from when the gas production drops the following years. Comparing this development with AMAP2011, also presented in Figure 3.1, gives the same trend of gas production as predicted from the Statfjord field even though the actual values differ. This is an indication of a 2D simulation model which is representative.

### 3 BASE CASE

---

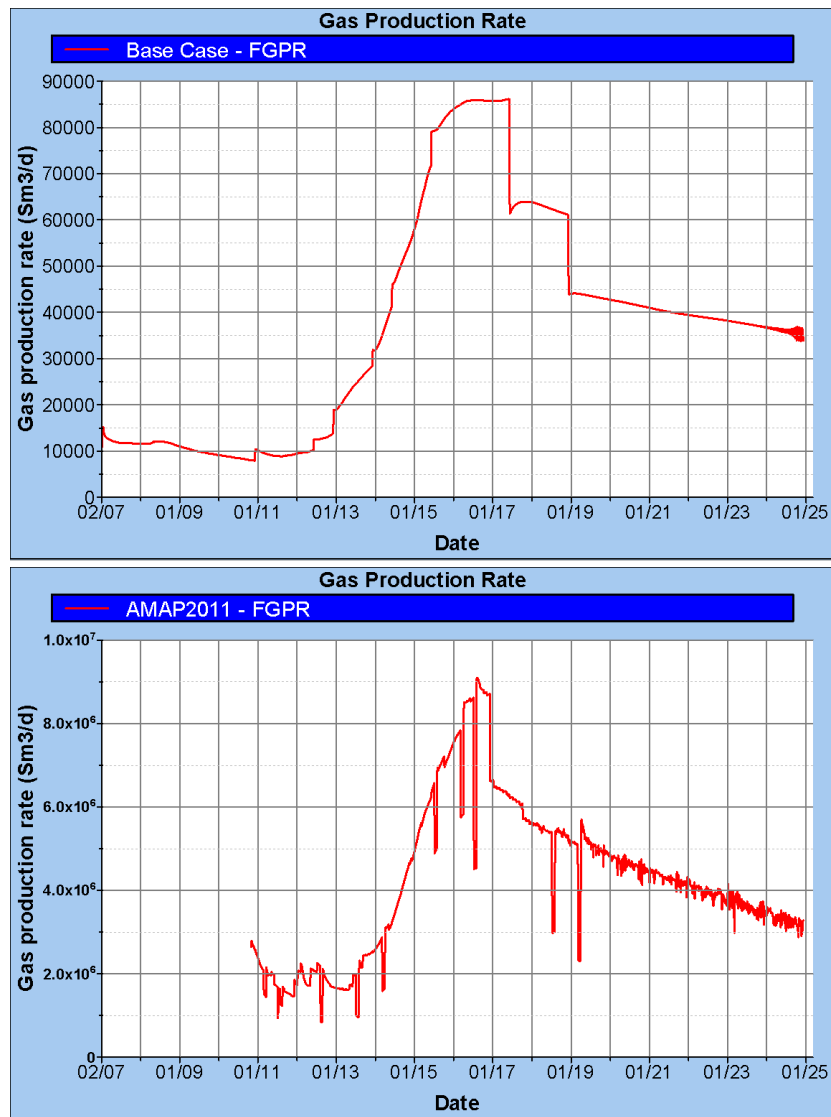


Figure 3.1: *Top plot:* The development of total gas production rate in the BASE CASE simulation run. *Bottom plot:* The development of total gas production rate in the AMAP2011 simulation run.

The same trend in development is observed in the two simulations, indicating a representative simplified model. FGPR is the field gas production rate, and reflects the total gas production rate from the field.



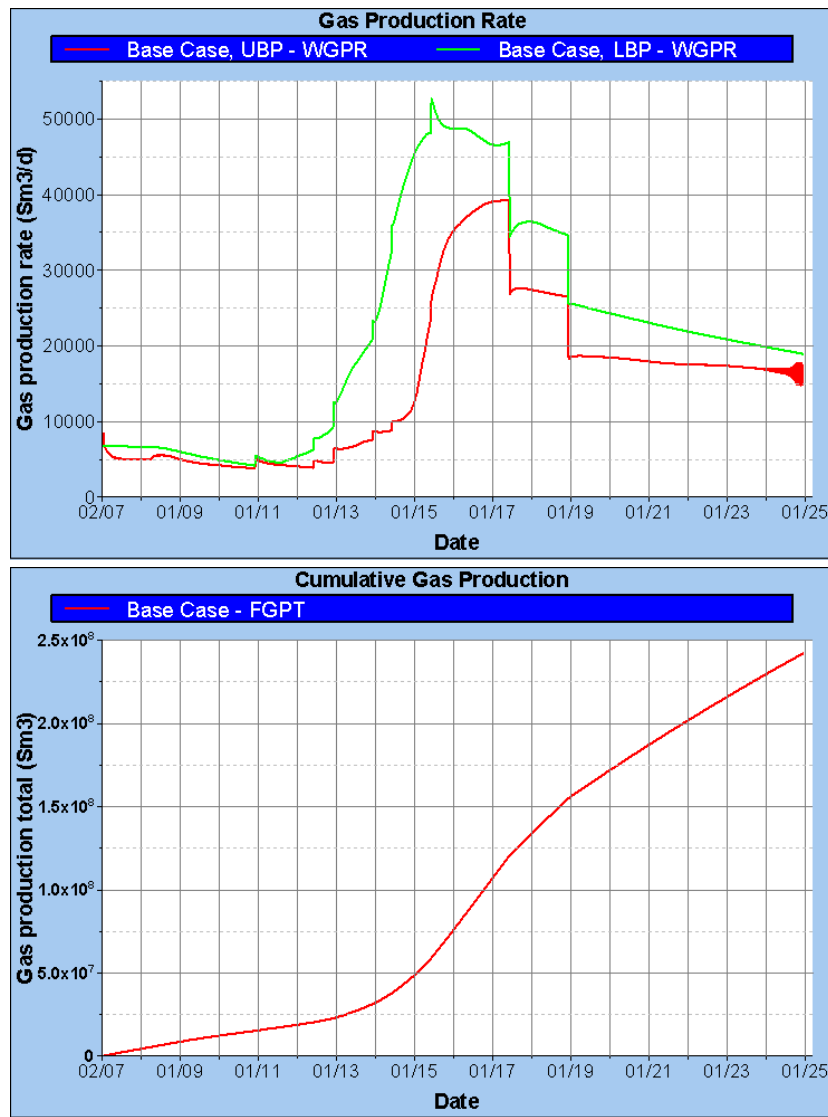


Figure 3.2: *Top plot:* The development of gas production rate from each well in the BASE CASE simulation run. *Bottom plot:* The development of total cumulative gas production in the BASE CASE simulation run.

The “gas bubble” is observed at an earlier stage in LBP, which is expected. WGPR is the gas production rate in the respective well. FGPT is the total cumulative gas production from the field.

If the well gas production rate (WGPR) for both UBP and LBP is plotted through time, as presented in Figure 3.2, it becomes obvious that the “gas bubble” is first observed in Lower Brent. This is expected since Lower Brent

### 3 BASE CASE

---

contains a larger amount of dissolved gas and will reach mobile gas phase at an earlier stage. Even though it is located deeper than Upper Brent and will reach the bubble point of the oil at a later stage, the larger amount of gas in place leads to an earlier production of the “gas bubble”. It is also obvious that the main contributor to the gas production is LBP.

*Field gas production total* (FGPT) is the cumulative gas production from both UBP and LBP, presented in Figure 3.2. Plotted through time, the “gas bubble” is observed as a faster increase in FGPT. The cumulative gas production is observed at about  $2.42 \cdot 10^8 \text{ Sm}^3$  when the simulation ends in year 2025. The values of cumulative gas produced and gas production rate are not of importance as a single value. The purpose of investigating the values is to observe the increase or decrease when introducing different changes to the BASE CASE.

## 4 Base Case with refined East Flank grid (BASE CASE REF)

The focus of this thesis is upscaling of the Main Field. However, the BASE CASE includes grid blocks of the East Flank, as shown in Figure 4.1 with grid blocks assigned colors from pink to yellow.

### 4.1 Modification

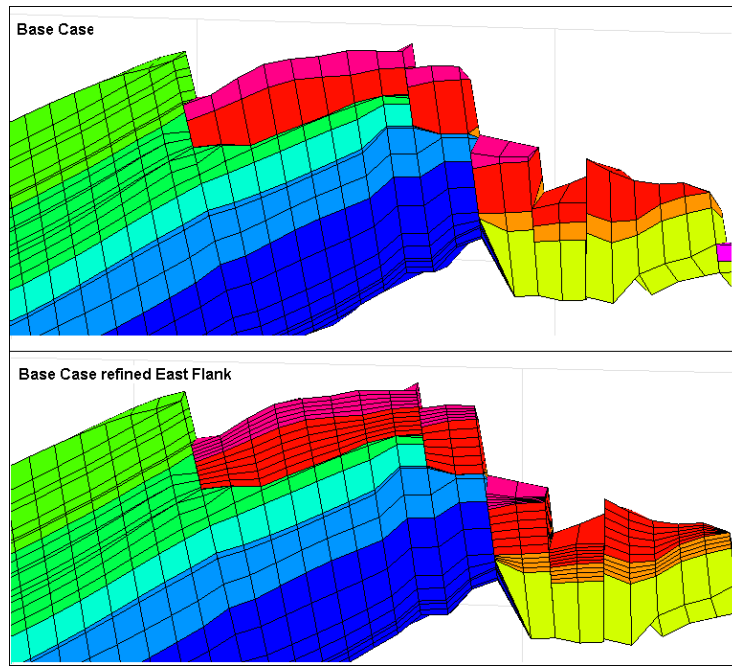


Figure 4.1: The difference of grid between BASE CASE without (*top image*) and BASE CASE REF with (*bottom image*) refined grid in the East Flank. Main Field is recognized by the colors from green to deep blue, while the East Flank is recognized by the colors from pink to yellow. East Flank cells with neighbor cells in Main Field is refined in the BASE CASE REF.

The effect of liberated gas flowing in thin layers with high mobility will also be present in the East Flank. Gas liberated in the East Flank will affect the production from the Main Field, due to communication through the faults. In order to study the gas flow in the whole reservoir with respect to this effect, the East Flank coarse grid is refined. This refinement will give increase in gas flow from the East Flank without having to calculate and upscale the gas relative permeability in the BASE CASE East Flank. Cells in East Flank with neighbor cells in the Main Field are refined from having a height in the range 10-25

## 4 BASE CASE WITH REFINED EAST FLANK GRID (BASE CASE REF)

---

meters, to having a height in the range 2-5 meters. This modified version of the BASE CASE will be referred to as the BASE CASE REF. The range is considered to be adequate by later discussion in the thesis. The refined grid is compared visually with the BASE CASE grid in Figure 4.1, and the refined East Flank will be kept in all later modifications of the model unless otherwise described. A table is presented in Figure A.3 on page 77 which is an overview over the layers in the East Flank in the different simulation models in this thesis, and helps understand the dividing and combining of the cells. The layers in the overview is presented with  $\bar{k}$  value, and all later references to layer numbers will be according to this figure.

### 4.1.1 RESVIEW divide command

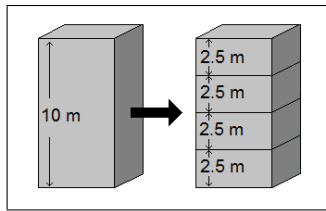


Figure 4.2: A visualization of the RESVIEW divide command

The refining of the East Flank coarse grid from the BASE CASE is done by using RESVIEW. The BASE CASE grid is loaded together with all belonging cell parameters (both initial and restart parameters). RESVIEW provides a command called “divide” in “edit grid” mode. If this command is called for the XY plane, it will require input of a Z value (from-to), which defines which layer(s) is to be divided. The command also requires a number of how many new layers this defined original layer will be divided into. When the values have been defined, RESVIEW will divide the defined layer into the desired number of new layers with an equal height of all new layers (a visualization is shown in Figure 4.2). The dividing will be applied to the entire layer. This command will also assign all initial parameters to all new cells equal to the initial parameters of the cell divided.

The problem with the divide command is that RESVIEW do not allow editing of the grid when restart parameters are loaded. Assigning restart parameters to the new cells equal to the restart parameters of the cell divided must be carried out. A simple method to make this possible is to copy all restart parameters of original grid to be loaded and read as initial parameters. Hence, they will also be assigned to all new cells when using the “divide” function.

The problem with the divide command is that RESVIEW do not allow editing of the grid when restart parameters are loaded. Assigning restart parameters to the new cells equal to the restart parameters of the cell divided must be carried out. A simple method to make this possible is to copy all restart parameters of original grid to be loaded and read as initial parameters. Hence, they will also be assigned to all new cells when using the “divide” function.

After editing the grid and parameters with RESVIEW, grid is exported together with initial and restart parameters as files containing keywords for ECLIPSE simulation. Before simulation is possible to carry out, the same preparations as described in subsection 2.2 on page 26 must be applied.

Fluid data and saturation functions from the BASE CASE are unchanged. This will not be in conflict with the cells added, as they inherit the SATNUM value from the original cell divided.

## 4.2 Simulation results

The BASE CASE REF is simulated with ECLIPSE, and a visualization of the run is evaluated with FLOVIZ and S3GRAF. A 3D visualization of the grid with color scheme representing gas saturation (SGAS) is presented in Figure 4.3, and shows a comparison of gas saturation distribution at the last simulation time step (1 JAN 2025) from BASE CASE and BASE CASE REF.

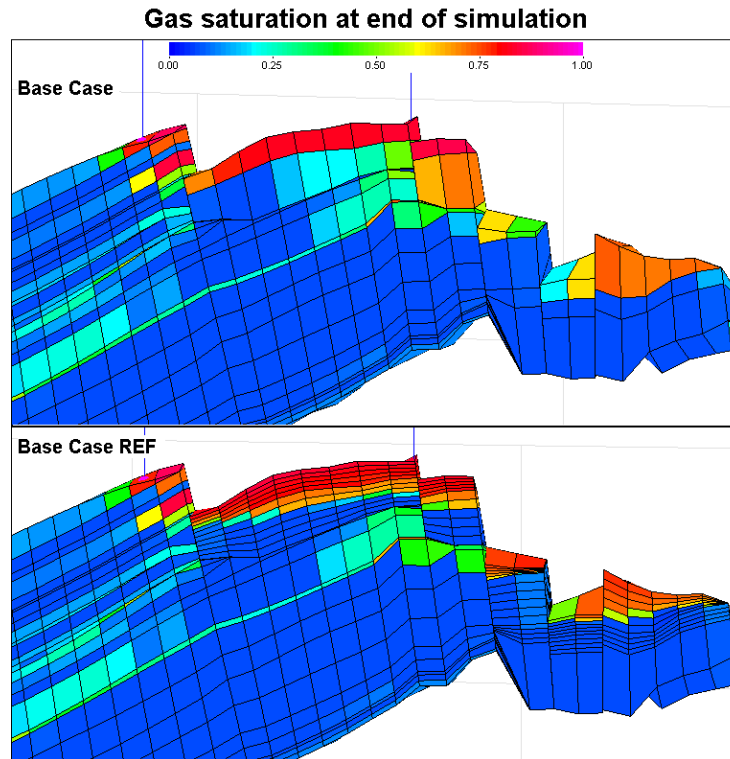


Figure 4.3: Comparison of BASE CASE (*top image*) and BASE CASE REF (*bottom image*) with respect to gas saturation distribution at the end of the simulations (1 JAN 2025). The color scheme represents the gas saturation. The effect of gas segregating to the top layers in the East Flank becomes very clear. The thin, high gas saturation layers will increase the flow of gas in the reservoir.

The two results seems to represent a very similar situation. However, when considering the “small” differences the thin top structure layers provide, the two simulations differs in gas flow and production. The BASE CASE REF allows ECLIPSE to simulate the gas saturation distribution more accurate. Instead of considering a large cell with a low overall gas saturation, thin cells located in top of the area covered by a large cell will receive a high gas saturation. The thin cells located in the lower area covered by a large cell will allow the gas to

#### **4 BASE CASE WITH REFINED EAST FLANK GRID (BASE CASE REF)**

---

segregate out, giving a very small gas saturation. Considering the gas relative permeability, the low average gas saturation in the large cells from BASE CASE will imply less flow than the few upper cells of the same area in the BASE CASE REF with high gas saturation.

To consider the effect on gas production by refining the East Flank, plots are created in S3GRAF to compare BASE CASE and BASE CASE REF. In Figure 4.4, the gas production rate through time is presented both on the basis of total production and separated into production wells for the two simulation runs. The total gas production rate is affected by the refining of the East Flank and shows an increase at the peak of the “gas bubble”. If closer investigated, the peak of the “gas bubble” will increase about 8 %, from about 86,000 Sm<sup>3</sup>/d to 93,000 Sm<sup>3</sup>/d, at the most. The period of increased gas production rate is observed to last from about mid 2014 until about mid 2017, which yields a period of about 3 years. However, the timing of the “gas bubble” is not affected, only the amount of gas produced.

If the gas production rate is considered separated into production wells, it is obvious that the increased production originates from LBP. The production rate of UBP does in fact decrease at the peak of the “gas bubble”, and remains decreased throughout the simulation period. However, the decreased rate in UBP is small compared to the increase in LBP. The result of decreased gas production rate in UBP and increased gas production rate in LBP may be caused by the flow pattern of the gas in the reservoir. The refined grid allows more of the gas in place in the East Flank to migrate towards LBP and less gas to migrate towards UBP.

Figure 4.5 compares the two simulations with respect to cumulative gas production. When the simulation ends in 2025, the cumulative gas production in the BASE CASE is observed to be  $2.42 \cdot 10^8$  Sm<sup>3</sup>. Considering the refinement of the East Flank in the BASE CASE REF, this amount is increased to about  $2.49 \cdot 10^8$  Sm<sup>3</sup>. The result indicates an 3 % underestimation of the gas produced in the BASE CASE.

#### 4 BASE CASE WITH REFINED EAST FLANK GRID (BASE CASE REF)

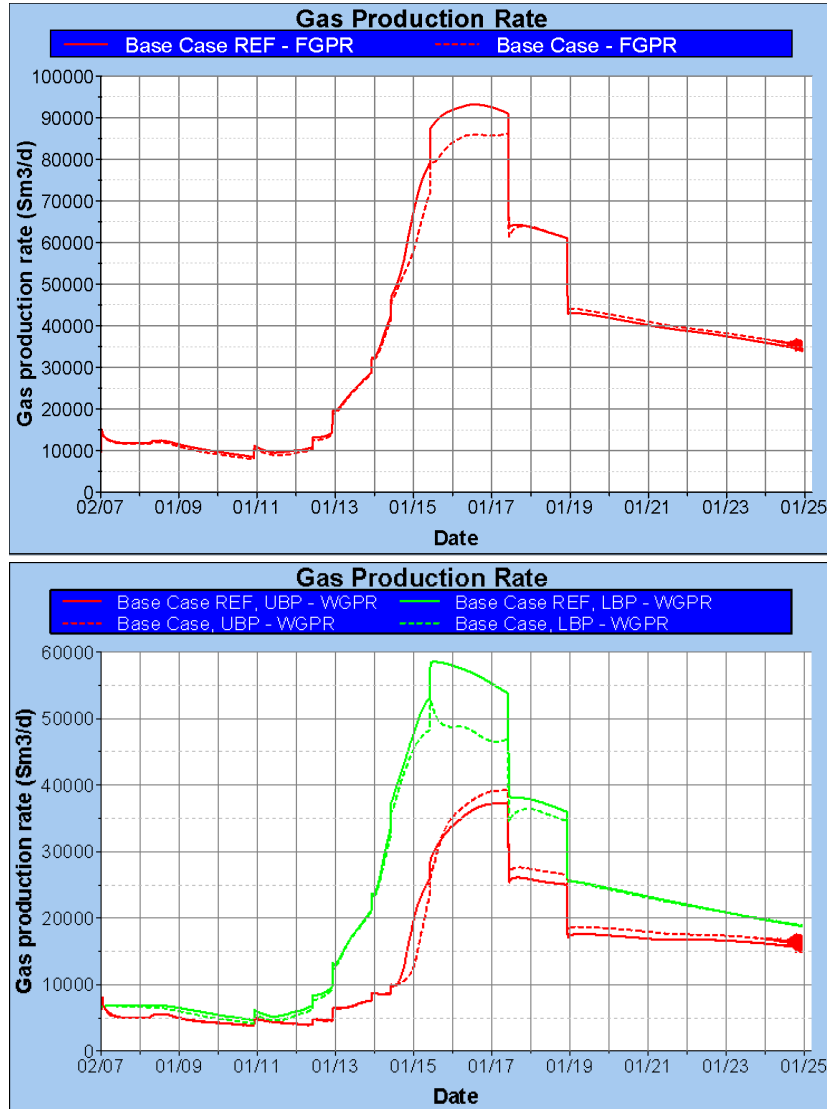


Figure 4.4: *Top plot:* The development of total gas production rate in the BASE CASE REF simulation run compared with the BASE CASE. *Bottom plot:* The development of gas production rate from each well in the BASE CASE REF simulation run compared with the BASE CASE.

The effect of refining the grid in the East Flank is observed as an 8 % increase in total gas production rate at the peak of the observed “gas bubble”. If the gas production is divided into wells, the increased gas production rate is observed to originate from LBP. However, the timing of the “gas bubble” is not affected.

**4 BASE CASE WITH REFINED EAST FLANK GRID  
(BASE CASE REF)**

---

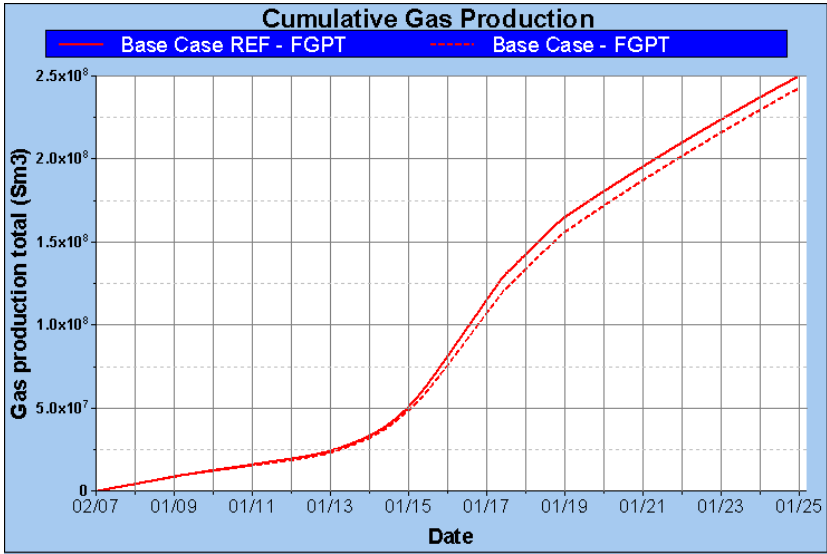


Figure 4.5: The development of total cumulative gas production in the BASE CASE REF simulation run compared with the BASE CASE. The effect of refining the grid in the East Flank is observed as an 3 % increase in cumulative gas production.



## 5 Refined Main Field grid (RMF 1)

Using BASE CASE REF as basis, the model is now prepared for modifications of the grid in the Main Field. This first model with refined grid in the Main Field will be referred to as the RMF 1. An overview of the grid/layer modifications of the Main Field in the different models is presented in Figure A.4 on page 78. The layers in the overview is presented with  $\vec{k}$  value, and all later references to layer numbers will be according to this figure.

### 5.1 Modification

If Figure 5.1 is studied with respect to the ability to accumulate thin layers of gas in the top part, four layers in the BASE CASE REF have been found to be good candidates for refining the grid. The layers with a value of zero transmissibility in the Z-direction represents a vertical flow barrier, and gas will accumulate below the barrier.

The upper layer indicated with an arrow (layer 19) is chosen because the boundary condition on top of it plays the role as a vertical flow barrier. The layer indicated by the second arrow from the top (layer 22) is chosen because it is located directly below a vertical flow barrier. The layer indicated by the third arrow from the top (layer 28) is chosen to observe the effect of refining a layer which is observed from Figure 5.1 and 4.3 to accumulate gas, even though it plays the role as a vertical flow barrier. The layer indicated by the bottom arrow (layer 38) is chosen to observe the effect of refining the grid just below the thin layer in Lower Brent, which seems to already be adequate for simulating the effect of the thin gas bearing layer below a vertical flow barrier. The individual layers are divided into new layers having a height of approximately 2 meters using the divide function in RESVIEW. A visualization of the refinement from BASE CASE REF to RMF 1 is shown in Figure 5.2. After the refining of the Main Field is carried out, the grid and parameters are exported from RESVIEW as input files for simulation with ECLIPSE. Before simulation is possible to carry out, the same preparations as described in subsection 2.2 on page 26 must be applied.

Fluid data and saturation functions from the BASE CASE are unchanged. This will not be in conflict with the cells added, as they inherit the SATNUM value from the original cell divided.

## 5 REFINED MAIN FIELD GRID (RMF 1)

---

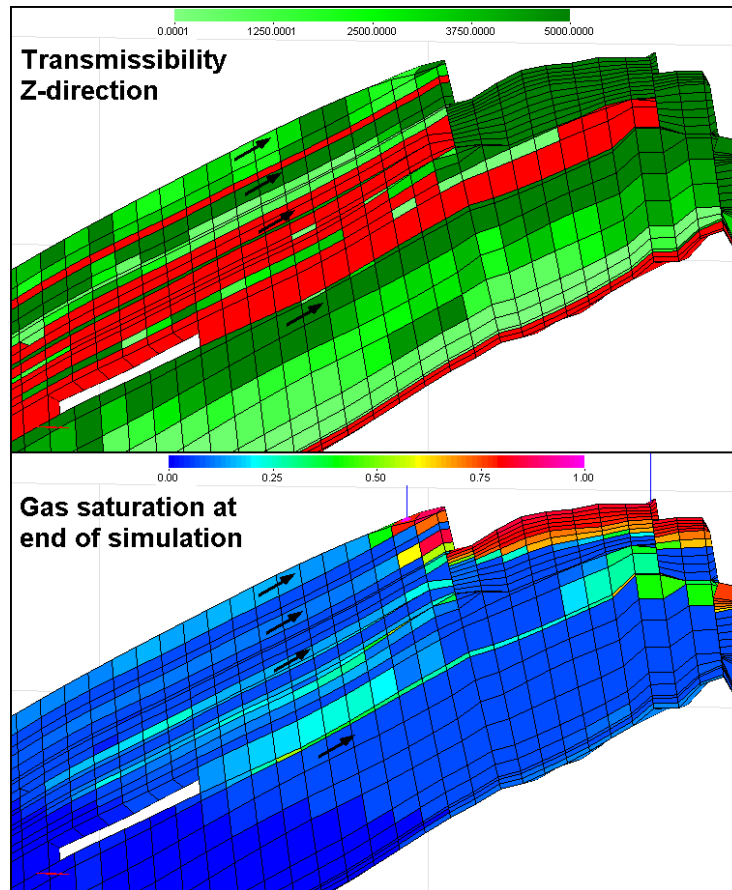


Figure 5.1: Analysis of BASE CASE REF for choosing candidate layers for refining. Top image shows the transmissibility in Z-direction, where the color red represents the value zero. Other values are represented by the color scheme. Bottom image shows the gas saturation at the end of the simulation (1 JAN 2025). Arrows indicate candidate layers.

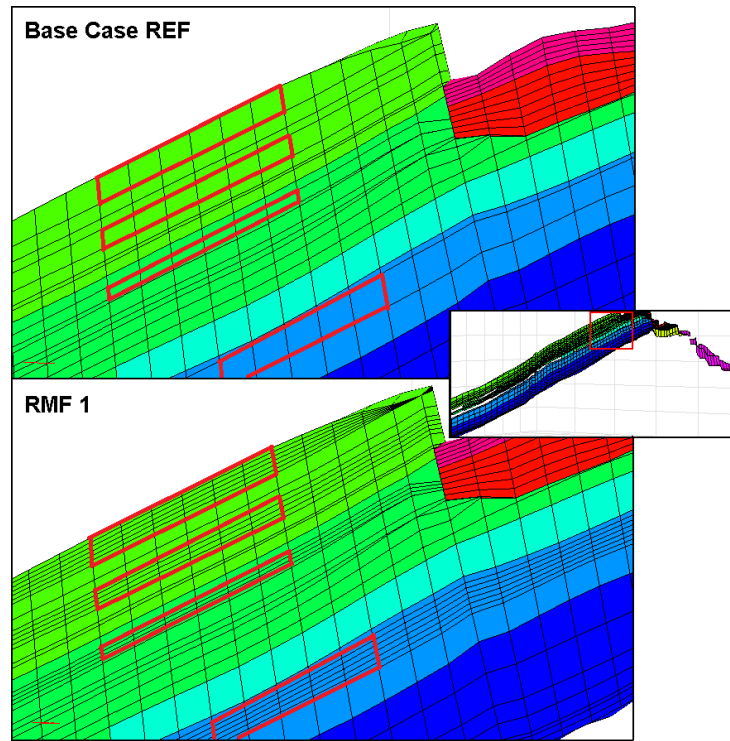


Figure 5.2: The grid difference between BASE CASE REF (*top image*) and RMF 1 (*bottom image*). Main Field is recognized by the colors from green to deep blue, while the East Flank is recognized by the colors from pink to red. East Flank is only visible in the top right corner of the images.

Layers to be refined are chosen with respect to the ability to accumulate gas in the top part. Layers 19, 22, 28 and 38 are divided into 6, 4, 3 and 6 new layers respectively.

## 5.2 Simulation results

The RMF 1 is simulated with ECLIPSE, and a visualization of the run is evaluated with FLOVIZ and S3GRAF. A 3D visualization of the grid with color scheme representing gas saturation (SGAS) is presented in Figure 5.3, and shows a comparison of gas saturation distribution at the last simulation time step (1 JAN 2025) from BASE CASE REF and RMF 1. The comparison gives the same result as observed when refining the East Flank, the gas flows vertically upwards and accumulates. The existence of vertical flow barriers separates the general result in the Main Field from what was observed when refining the East Flank. The flow barriers generate several layers in the reservoir where gas can accumulate and develop high gas mobility, demonstrated clearly by the second layer from the top which was refined. Observing the third layer from the top which was refined, the effect of gas moving vertically is not present. This was

## 5 REFINED MAIN FIELD GRID (RMF 1)

---

expected as the layer has zero transmissibility in Z-direction, and the refinement does not affect the gas production. A more interesting observation, is the lower most refinement located in Lower Brent. If the figure is investigated in detail, a slight increase in gas saturation is observed in the top of the new layers quite low in the reservoir. The increase in gas saturation originates from the fact that one single cell in the layer above, where the gas is observed to accumulate, has a very low absolute permeability. The gas flowing in the high saturated layer is “forced” down in the refined layer, passing this cell of low absolute permeability.

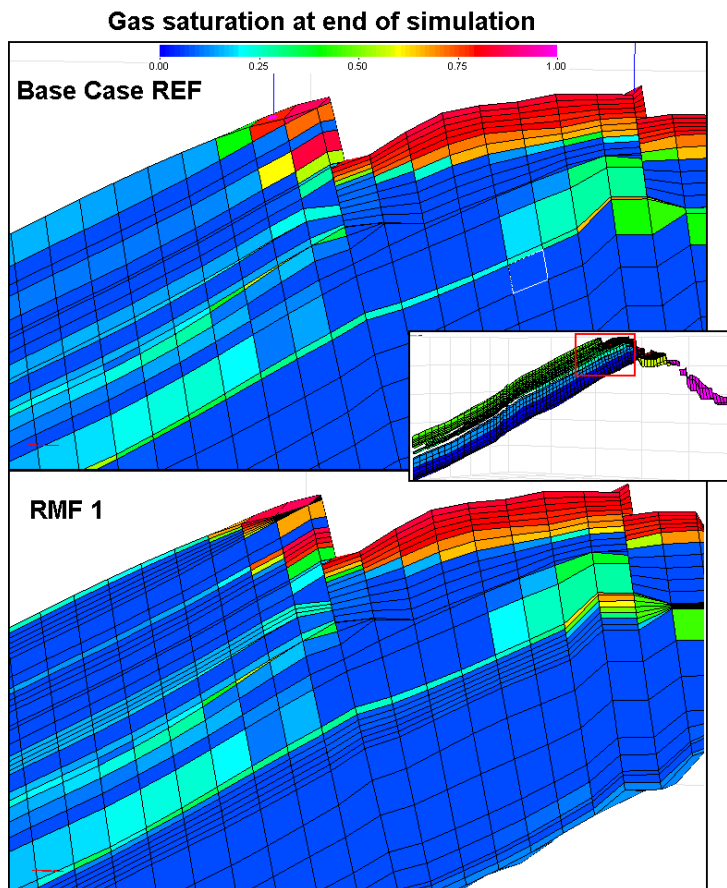


Figure 5.3: Comparison of BASE CASE REF (*top image*) and RMF 1 (*bottom image*) with respect to gas saturation distribution at the end of the simulations (1 JAN 2025). The color scheme represents the gas saturation.

The effect of gas segregating to the top layers in the Main Field becomes, as in Figure 4.3 East Flank, very clear. The thin, high gas saturation layers will increase the flow of gas in the reservoir. However, the refinement of layer 28 in BASE CASE REF is observed to have very little effect.

In order to investigate the effect of the gas production in greater detail, plots of the production rates are created using S3GRAF. Figure 5.4 shows a comparison of RMF 1 and BASE CASE REF with respect to both total gas production rate and gas production rate from each of the wells through time. In contrast with the observation from refining the East Flank, the timing of the “gas bubble” is affected, as it is not only governed by the pressure development. The thin layers where gas accumulates allow the gas to become mobile at an earlier time. The affected timing is most clearly observed in UBP. However, the refining again affects the peak of the “gas bubble”. BASE CASE REF is observed to peak at  $93,000 \text{ Sm}^3/\text{d}$  in total gas production rate, while the RMF 1 is observed to peak at  $99,500 \text{ Sm}^3/\text{d}$ . This yields a 7 % increase in total gas production rate at the peak. If the BASE CASE is considered, the refining of both East Flank and Main Field yield an 15.7 % increase in total gas production rate at the peak.

Considering the gas production rates from the separated wells, an increase is observed at the peak in both LBP and UBP. The increased gas production rate in Lower Brent may be caused by the refinement below the high saturated layer, which was an unexpected result. However, when investigating the saturation development close to the cell mentioned above with low absolute permeability, it is explained by the gas which is allowed to flow under and past the restriction given by this cell. The “small” amount of gas forced down in the layer below the high saturated layer will increase the saturation of the cell entered. If the cell entered has a large volume, the increase in saturation will be small and critical gas saturation is reached at a later stage or not overcome at all. When the cell entered has a smaller volume, the gas entered will have a larger impact on the saturation, and gas flow will occur at an earlier time.

The increase in gas production rate in UBP is expected when considering that the gas segregates to the top layer. When the total volume of the cells the gas enters in the top are smaller, the gas saturation becomes a larger value, and the relative gas permeability yields a larger gas flow.

The increase in total gas production rate is reflected in the total cumulative gas production from the simulations. Figure 5.5 shows a comparison of the total cumulative gas production of RMF 1 and BASE CASE REF. At the end of the simulations in year 2025, the RMF 1 simulation run gives a cumulative gas production of  $2.60 \cdot 10^8 \text{ Sm}^3$ , which is a 4 % increase from the  $2.49 \cdot 10^8 \text{ Sm}^3$  produced in the BASE CASE REF simulation run. If again, the BASE CASE is considered, the refining of both East Flank and Main Field yield an 7.4 % increase in total cumulative gas production.

## 5 REFINED MAIN FIELD GRID (RMF 1)

---

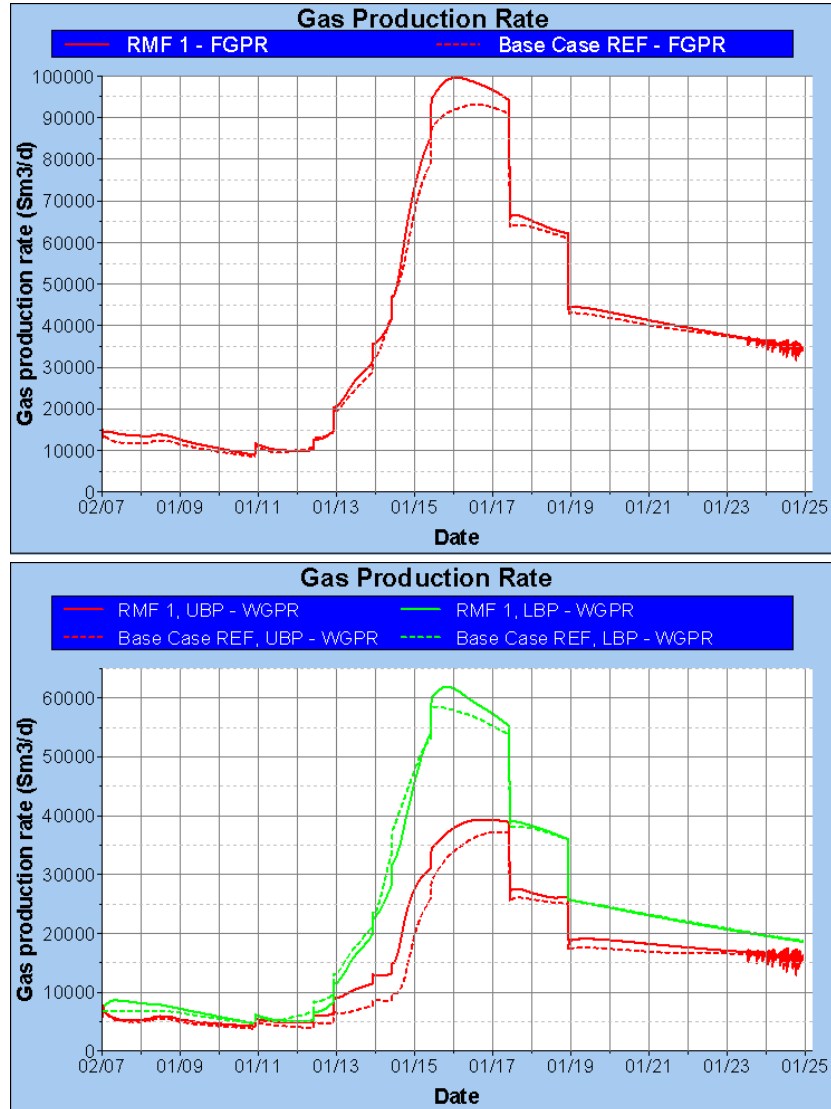


Figure 5.4: *Top plot:* The development of total gas production rate in the RMF 1 simulation run compared with BASE CASE REF. *Bottom plot:* The development of gas production rate from each well in the RMF 1 simulation run compared with BASE CASE REF.

The effect of refining the grid in the Main Field is observed as an 7 % increase in total gas production rate at the peak of the observed “gas bubble”. If the gas production is divided into wells, increase is observed at the peak in both UBP and LBP. The timing of the “gas bubble” is also affected.

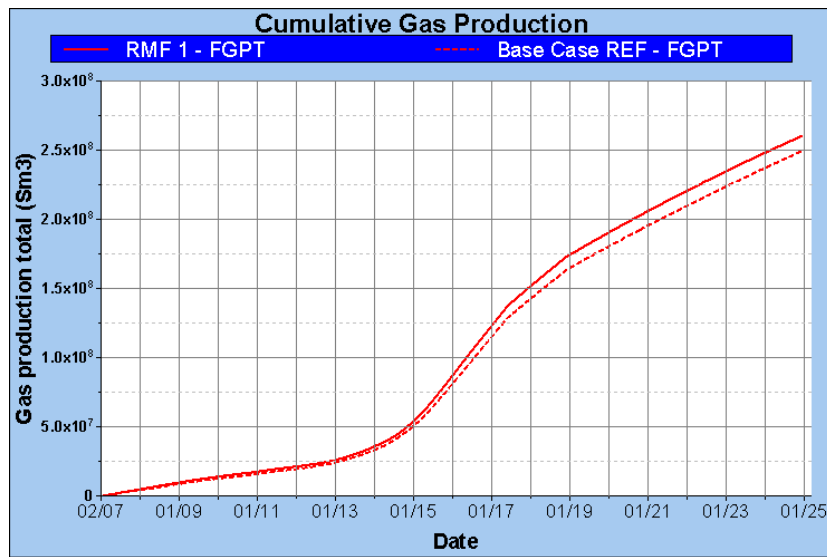


Figure 5.5: The development of total cumulative gas production in the RMF 1 simulation run compared with the BASE CASE REF run. The effect of refining the grid in the Main Field is observed as a 4 % increase in cumulative gas production.

**5 REFINED MAIN FIELD GRID  
(RMF 1)**

---



## 6 Refined Main Field grid (RMF 2)

Using RMF 1 as basis, the model is now prepared for further modifications of the grid in the Main Field. This second model with refined grid in the Main Field will be referred to as the RMF 2. An overview of the grid/layer modifications of the Main Field in the different models is presented in Figure A.4 on page 78. The layers in the overview is presented with  $\vec{k}$  value, and all later references to layer numbers will be according to this figure.

### 6.1 Modification

The RMF 1 was a refinement of four different layers in Main Field from BASE CASE REF (layers 19, 22, 28 and 38). To avoid confusion, it will from this point on be referred to refined zones 1,2, 3 and 4 (see Figure 6.1).

**Refined zone 1** is the zone which includes all the new layers created from the upper most layer in BASE CASE REF (layer 19) which was refined in RMF 1.

**Refined zone 2** is the zone which includes all the new layers created from the second layer which was refined in RMF 1 from the BASE CASE REF (layer 22), counting from the top.

**Refined zone 3** is the zone which includes all the new layers created from the third layer which was refined in RMF 1 from the BASE CASE REF (layer 28), counting from the top.

**Refined zone 4** is the zone which includes all the new layers created from the bottom layer which was refined in RMF 1 from the BASE CASE REF (layer 38).

Refined zone 3 proved to have little or none effect of gas segregating to the top, and will therefore be left unchanged in RMF 2. However, zone 1 and 2 were observed to allow the gas to segregate towards the top of the zones. In RMF 2 it is chosen to divide the top layer of the two zones further into another three new layers. The three new layers will have a height less than 1 meter. This is done to observe if this will affect the production and if the very thin layers are of adequate height so segregation effects will not influence the distribution of gas in the cells significantly.

Refined zone 4 was refined below a high gas saturated layer. In RMF 2 it is chosen to refine this high gas saturated layer above zone 4. The layer above zone 4 is also divided into three new layers, each having a height less than 1 meter.

A visualization of the refinement from RMF 1 to RMF 2 is shown in Figure 6.1

## 6 REFINED MAIN FIELD GRID (RMF 2)

---

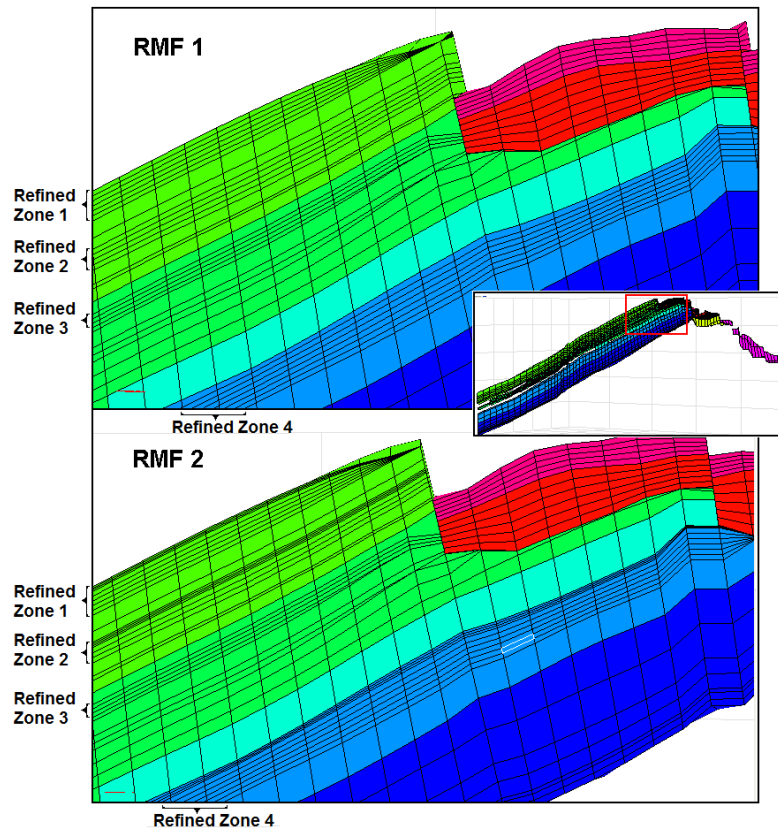


Figure 6.1: The grid difference between RMF 1 (*top image*) and RMF 2 (*bottom image*). Main Field is recognized by the colors from green to deep blue, while the East Flank is recognized by the colors from pink to red. East Flank is only visible in the top right corner of the images.

Main Field layers are further refined by dividing the top layers of the two already refined upper zones into three new layers. The third zone from the top which was refined from BASE CASE REF is unchanged. The bottom zone which was refined from BASE CASE REF is also unchanged. However, the layer directly above the bottom zone is refined by dividing it into three new layers.

After editing the grid and parameters with RESVIEW, grid is exported together with initial and restart parameters as files containing keywords for ECLIPSE simulation. Before simulation is possible to carry out, the same preparations as described in subsection 2.2 on page 26 must be applied.

Fluid data and saturation functions from the BASE CASE are unchanged. This will not be in conflict with the cells added, as they inherit the SATNUM value from the original cell divided.

## 6.2 Simulation results

The RMF 2 is simulated with ECLIPSE, and a visualization of the run is evaluated with FLOVIZ and S3GRAF. A 3D visualization of the grid with color scheme representing gas saturation (SGAS) is presented in Figure 6.2, and shows a comparison of gas saturation distribution at the last simulation time step (1 JAN 2025) from RMF 1 and RMF 2.

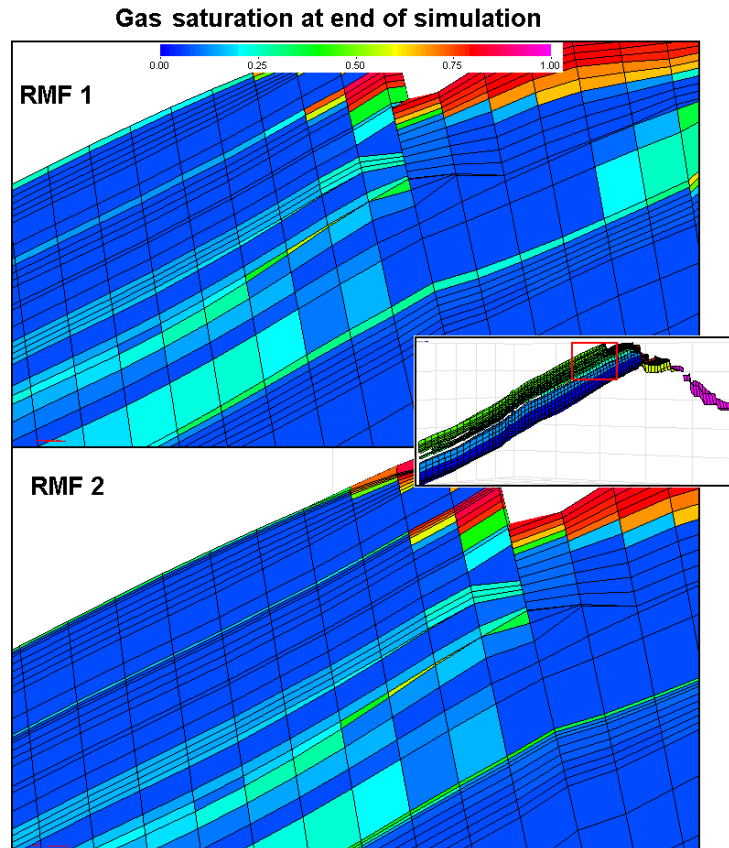


Figure 6.2: Comparison of RMF 1 (*top image*) and RMF 2 (*bottom image*) with respect to gas saturation distribution at the end of the simulations (1 JAN 2025). The color scheme represents the gas saturation.

The effect of gas segregating to the top layers in the Main Field is obvious. The thin, high gas saturation layers will increase the flow of gas in the reservoir. Gas coning is also observed in the vicinity of the well. However, this effect is not investigated in this thesis.

The vertical flow barriers become even more visible in refined zones 1, 2 and 4, and gas accumulates and flows in the thin layers located below these barriers.

## 6 REFINED MAIN FIELD GRID (RMF 2)

---

The representation of gas saturations in the figure indicate that even with a height less than 1 meter, it is an adequate thickness for the layers to contain all the gas in the Statfjord example. The layers in Lower Brent stand out as a special case. The restriction of a cell having a very low absolute permeability in the layer refined from RMF 1 (Layer 47 above refined zone 4), affects the gas flow by forcing the gas to pass this cell in the layers below. This is reflected visually by gas present in several layers, and not exclusively in the top layer (furthest down the center of the image).

Figure 6.3 shows a comparison of BASE CASE REF, RMF 1 and RMF 2 with respect to both total gas production rate and individual well gas production rates. Considering the two comparisons, RMF 1 and 2 seem almost identical. This indicates that the refinement in RMF 1 is adequate to include the effect of gas segregating upwards until vertical flow barriers create thin layers with high gas mobility. ECLIPSE will be able to simulate the effect using a cell/layer height of about 2 meters below vertical flow barriers. The results also implies, in this case, that layers with a cell height of less than 1 meter still is able to receive all the gas liberated. This is dependent of the amount of gas dissolved in the oil in place, size of reservoir and the rate of pressure decrease. Therefore it is not an universal assumption. The limit of how thick a layer must be to be able to receive all gas liberated is possible to establish by further refinement and simulation. However, this value is not of interest in this thesis, and will depend on the individual reservoir investigated. The thickness of a layer below a vertical flow barrier is recommended, in this scenario, set to about 2 meters in order to both include the effect of high gas mobility in the layer and to be able to receive all the gas liberated. If a significantly larger amount of liberated gas is expected, an investigation of the limit for the height of a layer is needed, for it to be able to receive all gas liberated. A significantly smaller amount of liberated gas will most likely not be expected, since it would not be a situation where this drainage strategy would not be preferred, and is a situation of theoretical interest only.

Figure 6.4 is a comparison of RMF 2, RMF 1 and BASE CASE REF with respect to total cumulative gas production. The total cumulative gas production is observed to be  $2.62 \cdot 10^8 \text{ Sm}^3$  at the end of simulation run RMF 2. Compared with the observed  $2.60 \cdot 10^8 \text{ Sm}^3$  from RMF 1, this is only a increase of less than 1 %. As indicated from the gas production rate in the two simulations, the refinement of the Main Field in RMF 1 seems to be adequate to simulate the effect of gas segregating upwards until vertical flow barriers create thin layers with high gas mobility. This also implies that Layer 47 in RMF 1 was adequately thin to simulate the effect of the thin, high gas mobility layer. Layer 47 in RMF 1 is the original layer 37 in BASE CASE REF, hence the increased gas production from Lower Brent is caused by the refinement of refined zone 4. It is caused by another effect than a thin, high gas mobility layer just below a vertical flow barrier and must be investigated further.

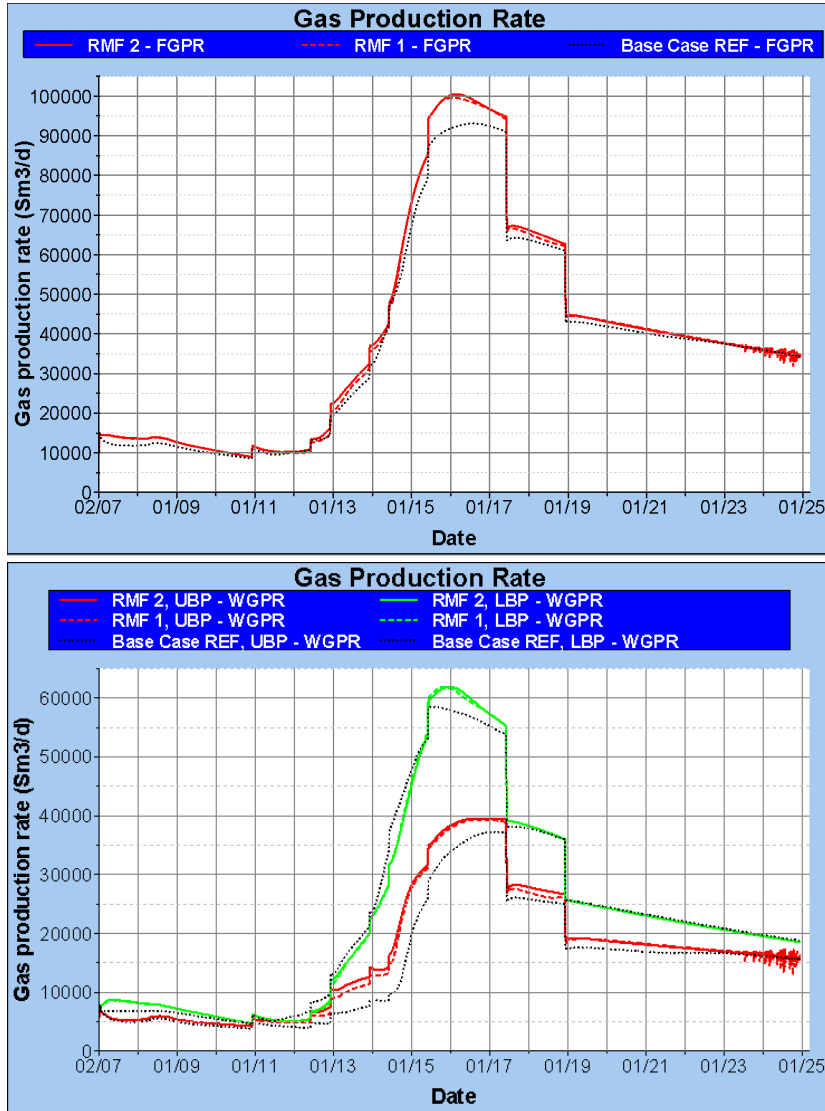


Figure 6.3: *Top plot:* The development of total gas production rate in the RMF 2 simulation run compared with RMF 1 and BASE CASE REF. *Bottom plot:* The development of gas production rate from each well in the RMF 2 simulation run compared with the RMF 1 and BASE CASE REF.

It is observed almost no change in the gas production rates, neither in total or individual well production, between RMF 2 and RMF 1. RMF 1 is adequate refined to include the effect of gas segregating upwards until vertical flow barrier creates thin layers with high gas mobility.

## 6 REFINED MAIN FIELD GRID (RMF 2)

---

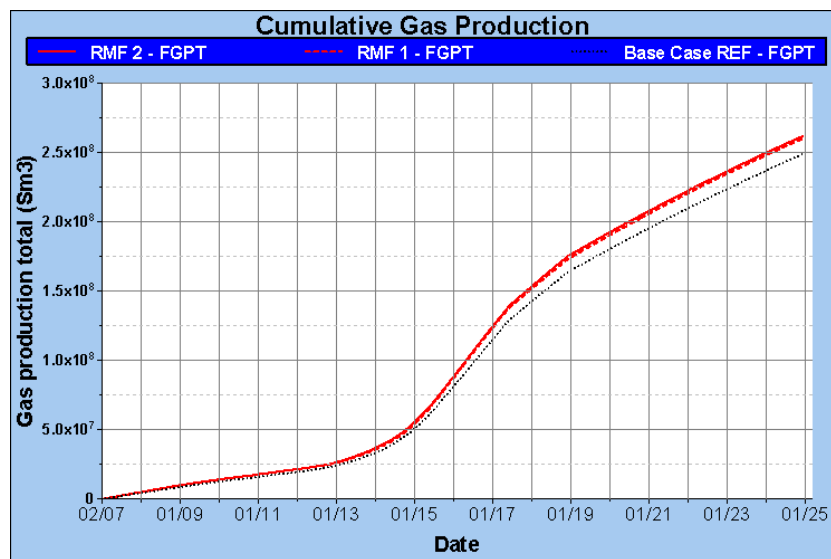


Figure 6.4: The development of total cumulative gas production in the RMF 2 simulation run compared with RMF 1 and BASE CASE REF.

The effect of refining the grid in the Main Field further is observed as a very small increase in cumulative gas production from RMF 1 to RMF 2. Less than 1 % increase. However, RMF 2 shows a 5 % increase in total cumulative gas production by refining the grid in Main Field.

## 7 Number of layers below vertical flow barriers

It has already been established in subsection 6.2 on page 49 that the thickness of a layer below a vertical flow barrier is recommended set to about 2 meters. In addition, the presence of a restriction in Lower Brent was discussed briefly, represented by low absolute permeability in the layer with high gas mobility. A sensitivity analysis of how the number of thin layers below vertical flow barriers affects the gas production is carried out in this section. The analysis consists of three different simulation models, which differs in grid dimensions in the Main Field. An overview of the grid/layer modifications of the Main Field in the different models is presented in Figure A.4 on page 78. The layers in the overview is presented with  $\vec{k}$  value, and all later references to layer numbers will be according to this figure.

### 7.1 Modification

A visualization of the three models created by modifying the grid in Main Field from RMF 2 is shown in Figure 7.1, and described in greater detail in the following sub subsections.

#### 7.1.1 Three thin layers below vertical flow barrier (SENS 3)

Layers 22-26 (in refined zone 1), 32-34 (in refined zone 2) and 54-59 (entire refined zone 4) from RMF 2 are combined, leaving only three thin layers below the vertical flow barriers (height less than 1 meter). The three refined layers above refined zone 4 differs from the three thin layers in top of zone 1 and 2. Above refined zone 4 they constitute the entire original layer 37 of the BASE CASE REF. Combining the entire refined zone 4 restores the original layer 38 of the BASE CASE REF.

The combining is done in RESVIEW with the command “combine” in “edit grid” mode. This command is the reverse of the “divide” command described in sub subsection 4.1.1 on page 34. However, the parameters inherited by the new single cell is an average value of the respective parameters assigned to the cells combined. In RMF 2, the refined zones are created by the “divide” command. Considering a single parameter when combining layers/cells, the average value assigned to the new single cell will then be equal to the value that was assigned to any of the cells combined.

Refined zone 3 (layers 40-41) from RMF 2 is also combined. This will restore the original layer 28 of the BASE CASE REF, and will not be investigated further since no effect of a layer with high gas mobility has been observed.

This configuration is referred to as the SENS 3 simulation model. After editing the grid and parameters with RESVIEW, grid is exported together with initial and restart parameters as files containing keywords for ECLIPSE simulation. Before simulation is possible to carry out, the same preparations as described in subsection 2.2 on page 26 must be applied.

## 7 NUMBER OF LAYERS BELOW VERTICAL FLOW BARRIERS

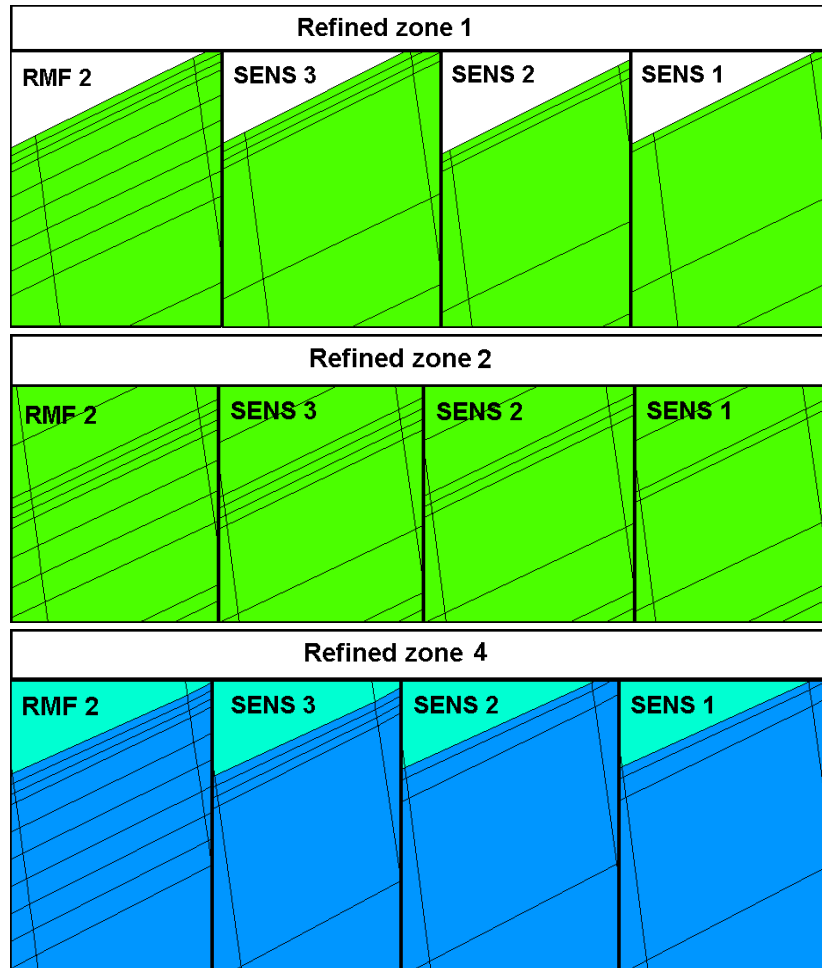


Figure 7.1: A visualization of modifications done in the Main Field grid considering the sensitivity analysis of the number of layers below a vertical flow barrier. The three refined layers above refined zone 4 in SENS 3 differs from the three thin layers in top of zone 1 and 2. Above refined zone 4 they constitute the entire original layer 25 from BASE CASE REF. There is no modification done above refined zone 4 from SENS 2 to SENS 1.



---

## 7 NUMBER OF LAYERS BELOW VERTICAL FLOW BARRIERS

---

Fluid data and saturation functions from the BASE CASE are unchanged. This will not be in conflict with the cells removed, as the new single cell inherit the SATNUM value from the cells combined.

### 7.1.2 Two thin layers below vertical flow barrier (SENS 2)

Layers 21-22 (in refined zone 1) and 27-28 (in refined zone 2) from SENS 3 are combined, leaving two thin layers below the vertical flow barriers (height less than 1 meter). Above zone 4, the layers 44-45 from SENS 3 is combined. This will only leave one single layer less than 1 meter below the vertical flow barrier. However, the second layer below the vertical flow barrier is only about 2 meters thick, and differs from the situation in refined zone 1 and 2.

This configuration is referred to as the SENS 2 simulation model. After editing the grid and parameters with RESVIEW, grid is exported together with initial and restart parameters as files containing keywords for ECLIPSE simulation. Before simulation is possible to carry out, the same preparations as described in subsection 2.2 on page 26 must be applied.

Fluid data and saturation functions from the BASE CASE are unchanged. This will not be in conflict with the cells removed, as the new single cell inherit the SATNUM value from the cells combined.

### 7.1.3 One thin layer below vertical flow barrier (SENS 1)

Layers 20-21 (in refined zone 1) and 25-26 (in refined zone 2) from SENS 2 are combined, leaving one single thin layer below the vertical flow barriers (height less than 1 meter). The configuration above refined zone 4 from SENS 2 is unchanged, and has only one single thin layer below the vertical flow barrier with height less than 1 meter.

This configuration is referred to as the SENS 1 simulation model. After editing the grid and parameters with RESVIEW, grid is exported together with initial and restart parameters as files containing keywords for ECLIPSE simulation. Before simulation is possible to carry out, the same preparations as described in subsection 2.2 on page 26 must be applied.

Fluid data and saturation functions from the BASE CASE are unchanged. This will not be in conflict with the cells removed, as the new single cell inherit the SATNUM value from the cells combined.

## 7.2 Simulation results

SENS 1,2 and 3 are simulated with ECLIPSE, and a visualization of the run is evaluated with FLOVIZ and S3GRAF. The visualization of the gas saturation with color scheme differs very little from the RMF 2 simulation run, and is distinguished mainly by the number of layers. No new observations can be

## ***7 NUMBER OF LAYERS BELOW VERTICAL FLOW BARRIERS***

---

drawn from it, other than that gas still segregates up into the thin layers below vertical flow barriers. The figure is therefore not included.

Investigating the effect of the modifications is done by using plots created with S3GRAF. Figure 7.2 shows a comparison of the total gas production rate and total cumulative gas production between RMF 2, BASE CASE REF, SENS 3, SENS 2 and SENS 1. Three different effects of the combining is observed when investigating the two plots.

The first observation is that SENS 1,2 and 3 seems to be quite similar both in total gas production rates and total cumulative gas production. Even if Figure 7.3 is investigated, with gas production rates from each well, this similarity is observed. The observation indicates that one single, adequately thin layer below a vertical flow barrier will allow ECLIPSE to simulate the effect. More than one layer is not needed. However, several thin layers do not affect the result.

The second observation is that a reduction in gas production rate is observed at the peak of the “gas bubble” going from RMF 2 to SENS 3. This can be explained if Figure 7.3 is taken into consideration. Figure 7.3 is a comparison of the gas production rates from each well between RMF 2, BASE CASE REF, SENS 3, SENS 2 and SENS 1. The reduction of total gas production rate originates from LBP. The only modification done to affect this well is the restored layer 38 of the BASE CASE REF, keeping layer 37 of the BASE CASE REF refined into three layers. The reduction of gas production rate is probably caused by the existence of the restriction from a cell with low absolute permeability in the three refined layers. As previously observed, this will force the gas to pass this cell in the underlying layer, which in SENS 3 is the restored layer 38 of the BASE CASE REF. The large height of this underlying layer causes the gas to loose mobility and the gas has to accumulate to continue flowing. Thus, the flow is restricted.

It is earlier stated that layer 37 of the BASE CASE REF was originally adequately thin to include the effect of increased gas production. Together with the observation that one single adequately thin layer will include the effect and that the same low absolute permeability restriction is present, it yields that little effect should be observed between BASE CASE REF and SENS 3 when considering the gas production rate in LBP. Investigating Figure 7.3, this similarity is confirmed as the third observation. Nevertheless, the total cumulative gas production from RMF 2, SENS 3, SENS 2 and SENS 1 shows an almost similar increase of about 4 % from the BASE CASE REF.

## 7 NUMBER OF LAYERS BELOW VERTICAL FLOW BARRIERS

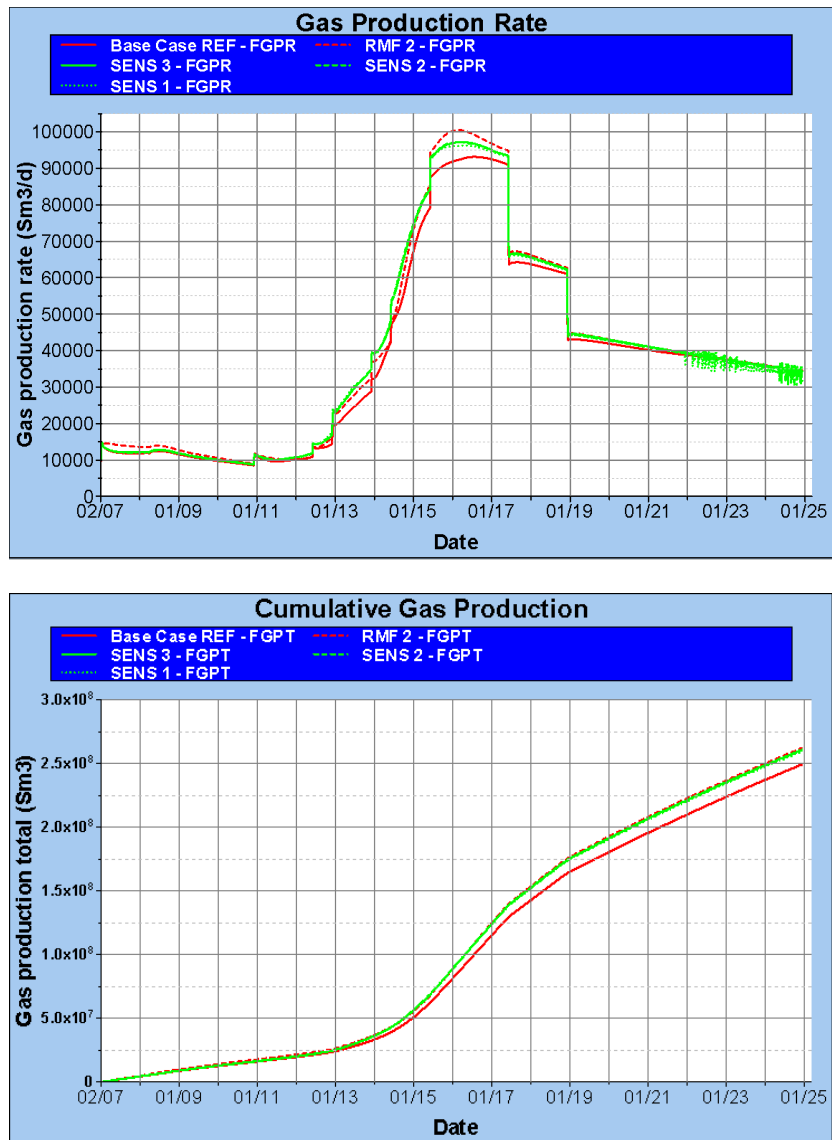


Figure 7.2: *Top plot:* The development of total gas production rate in the SENS 1,2 and 3 simulation runs compared with RMF 2 and BASE CASE REF. *Bottom plot:* The development of total cumulative gas production in the SENS 1,2 and 3 simulation runs compared with RMF 2 and BASE CASE REF.

The total gas production rate decreases from RMF 2 to SENS 1, 2 and 3 at the peak of the “gas bubble”. The total cumulative gas production does not differ significantly between RMF 2, SENS 1, 2 and 3, and is increased about 4 % from the BASE CASE REF simulation run. One single, adequately thin layer below a vertical flow barrier will include the effect of increased gas production.

## 7 NUMBER OF LAYERS BELOW VERTICAL FLOW BARRIERS

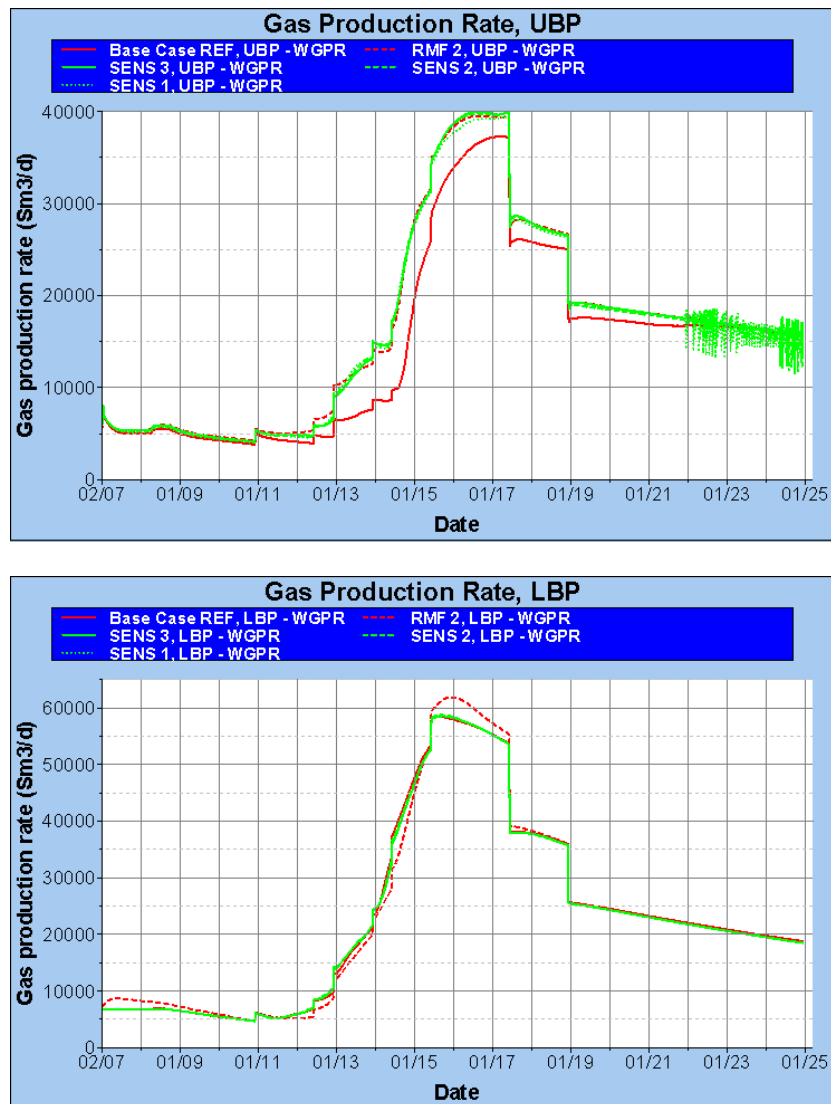


Figure 7.3: *Top plot*: The development of total gas production rate from UBP in the SENS 1,2 and 3 simulation runs compared with RMF 2 and BASE CASE REF. *Bottom plot*: The development of total gas production rate from LBP in the SENS 1,2 and 3 simulation runs compared with RMF 2 and BASE CASE REF.

The decrease in total gas production rate from RMF 2 to SENS 1, 2 and 3 originates from LBP. SENS 1, 2 and 3 have a quite similar gas production rate from LBP as BASE CASE REF, caused by a restriction in the high gas mobility layer combined with that BASE CASE REF originally has a single, adequately thin layer in Lower Brent.

## 8 Upscaling relative gas permeability and critical gas saturation in Main Field

An increased gas production is caused by refining the grid in order to include the thin, high gas saturated layer created below vertical flow barriers. An upscaling procedure is given in subsection 1.4 on page 22 which will consider the increased gas flow from a coarse grid block.

RMF 2 is used as fine grid model. Analysis of gas production affected by the refinement is carried out in previous sections, and an upscaling to make the BASE CASE REF match the RMF 2 with respect to gas production is carried out in this section.

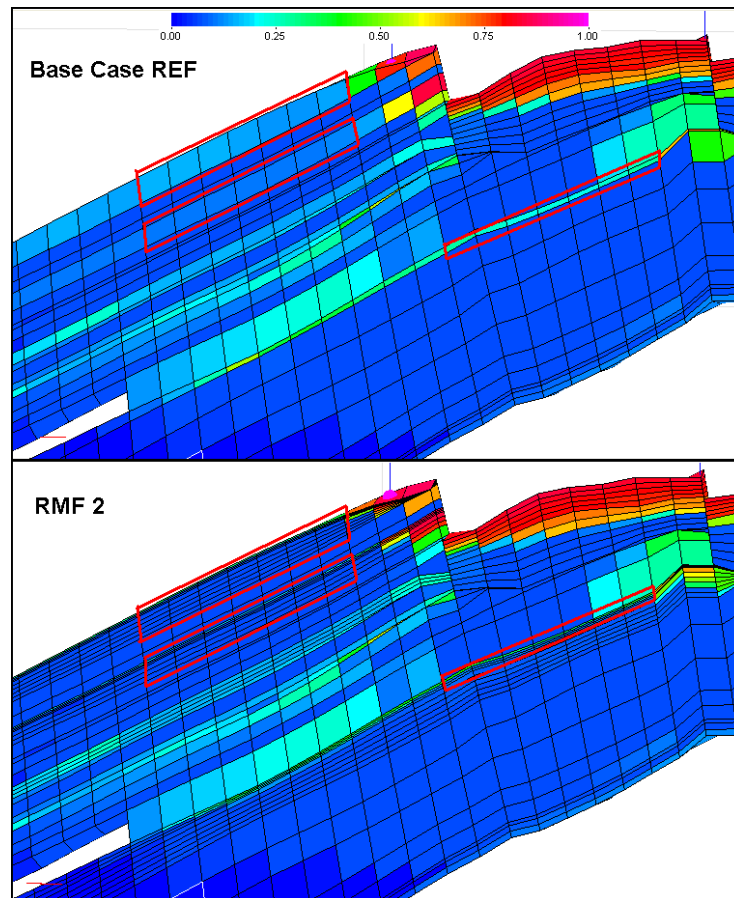


Figure 8.1: The cells chosen to calculate a transmissibility weighted average relative permeability from RMF 2 (*bottom image*) and the corresponding cells in BASE CASE REF (*top image*). The chosen cells are marked by red rectangles.

## 8 UPSCALING RELATIVE GAS PERMEABILITY AND CRITICAL GAS SATURATION IN MAIN FIELD

RMF 2 is simulated with ECLIPSE writing files containing gas saturations, relative permeabilities,  $NTG$ ,  $\Delta y$ ,  $\Delta z$  and pore volumes. The values are written at each time step for a selection in X-direction of seven cells in refined zone 1, seven cells in refined zone 2 and seven cells above refined zone 4. The selection is visualized in Figure 8.1. Layers 19-26 in RMF 2 (refined zone 1), corresponds to layer 19 in BASE CASE REF. Layers 29-34 in RMF 2 (refined zone 2), corresponds to layer 22 in BASE CASE REF. Layers 51-53 in RMF 2 (above refined zone 4), corresponds to layer 37 in BASE CASE REF. See overview in Figure A.4 on page 78.

The layer above refined zone 4, has already been pointed out to be adequately thin to include the effect of increased gas production. If an increase in gas production from Lower Brent should be obtained by upscaling the BASE CASE REF, refined zone 4 should be upscaled instead, even though refined zone 4 is not the layer located directly below the vertical flow barrier. This is due to the earlier mentioned restriction in the layer above refined zone 4. It is likely that this restriction is local, and if a 3D situation is considered, the gas may be able to flow around this restriction, and not be forced down into refined zone 4. Due to this, the selection above refined zone 4 is selected for the upscaling. This is done to observe if an upscaling will increase the gas production in the layer which is already adequately thin in the BASE CASE REF.

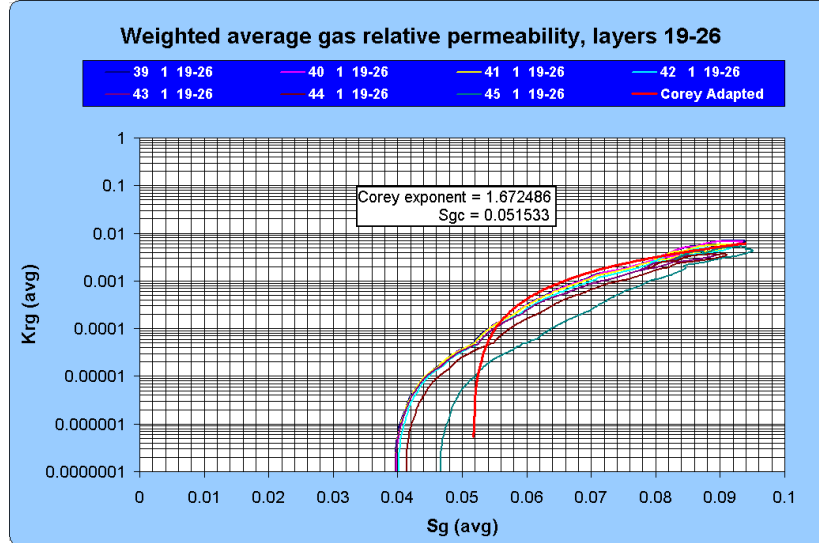


Figure 8.2: Transmissibility weighted average relative gas permeability plotted against pore volume weighted average saturation for the selection of cells in RMF 2 in refined zone 1. A normalized Corey relative permeability curve is adapted to be an average using the least square method, by varying the Corey exponent and critical gas saturation. The displayed Corey curve is denormalized.

## 8 UPSCALING RELATIVE GAS PERMEABILITY AND CRITICAL GAS SATURATION IN MAIN FIELD

Using the values written from the simulation and calculating equations 1.11, 1.12, 1.13 and 1.14, plots are created and upscaling performed. The transmissibility weighted average relative gas permeability is plotted against pore volume weighted average gas saturation in Figure 8.2 for the layers in refined zone 1. The normalized Corey relative permeability curve is found using the least square method together with the “solver” function in EXCEL by varying the Corey exponent and critical gas saturation, and finding the best match. The best match Corey relative permeability curve presented in Figure 8.2 seems to differ greatly from the observed permeabilities. This can be explained by the fact that the majority of the data observed is located in the saturation interval where the curves seems to be consistent. The least square method favors minimal difference in intervals where the majority of observed data exist. The simplicity of the Corey relation limits the form a curve can take. As a result of these factors, the best match curve differs greatly in some saturation intervals which has less data points. A table with the result of the “solver” function is presented in Table A.2 on page 80, together with the obtained normalized Corey relative gas permeability table, which is used as input to ECLIPSE for layer 19 in the BASE CASE REF UPSC simulation run (next section). Calculations made for the layers in refined zone 2 and above refined zone 4 is presented as plots in Figure 8.3 and 8.4 respectively.

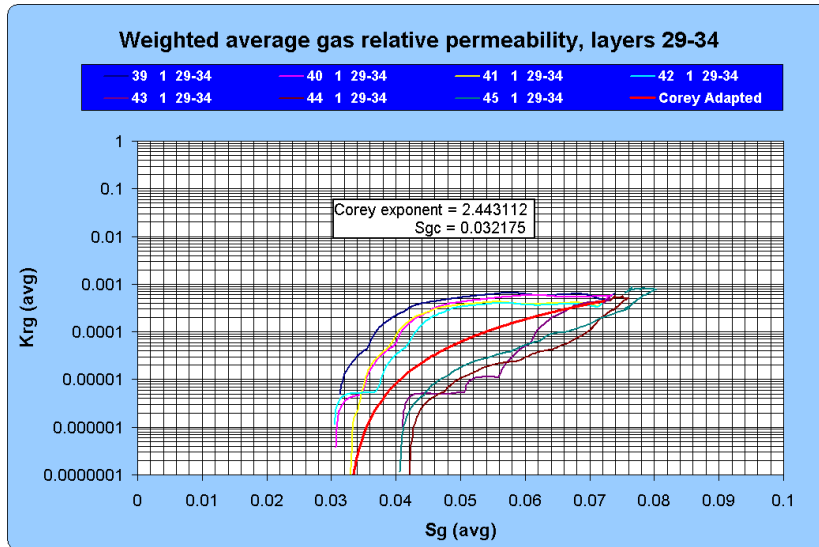


Figure 8.3: Transmissibility weighted average relative gas permeability plotted against pore volume weighted average saturation for the selection of cells in RMF 2 in refined zone 2. A normalized Corey relative permeability curve is adapted to be an average using the least square method, by varying the Corey exponent and critical gas saturation. The displayed Corey curve is denormalized.

## 8 UPSCALING RELATIVE GAS PERMEABILITY AND CRITICAL GAS SATURATION IN MAIN FIELD

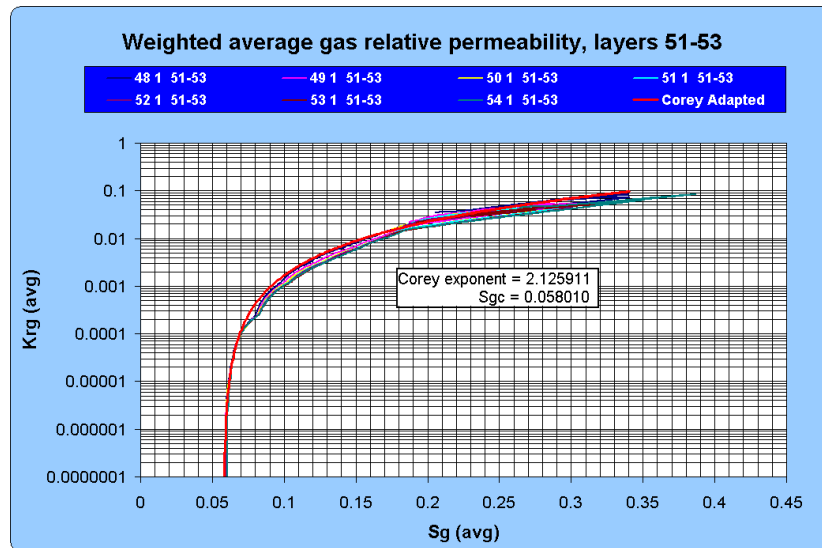


Figure 8.4: Transmissibility weighted average relative gas permeability plotted against pore volume weighted average saturation for the selection of cells in RMF 2 above refined zone 4. A normalized Corey relative permeability curve is adapted to be an average using the least square method, by varying the Corey exponent and critical gas saturation. The displayed Corey curve is denormalized.

Tables containing the result of the “solver” function for refined zone 2 and above refined zone 4 is presented in Table A.3 on page 81 and A.4 on page 82. The tables also include the obtained normalized Corey relative gas permeability table, which is used as input to ECLIPSE for layer 22 and 37 in the BASE CASE REF UPSC simulation run.



## **9 BASE CASE REF with upscaled parameters in Main Field (BASE CASE REF UPSC)**

Upscaled normalized Corey relative gas permeability curves for layers 19, 22 and 37 in BASE CASE REF have been created in section 8. As pointed out in subsection 1.4 on page 22, using these curves yields modification of the input critical gas saturation and saturation numbers for the respective layers. This upscaled version of the BASE CASE REF simulation model will be referred to as the BASE CASE REF UPSC simulation model.

### **9.1 Modification**

The grid in the upscaled model will be the same as used in the BASE CASE REF simulation run. However, the three new normalized Corey relative gas permeability tables presented in Tables A.2, A.3 and A.4 are added in the file containing the keyword SGFN, as table numbers 12, 13 and 14 respectively. The file containing the keyword SATNUM (saturation number) controls which relative permeability curves are to be used for each grid block, and must be modified for ECLIPSE to use the new curves. Saturation number for layer number 19 in BASE CASE REF UPSC is modified to the number 12, layer 22 is set to the number 13 and layer number 37 is set to the number 14. Relative permeability tables for oil and water must also contain tables number 12, 13 and 14. The tables of relative oil and water permeabilities originally belonging to layers 19, 22 and 37 are copied and pasted as tables number 12, 13 and 14 in the files containing the keywords SOF3 and SWFN.

The critical gas saturation obtained for each of the upscaled layers have to be included in the file containing the keyword SGCR, which controls at which saturation the gas starts flowing in each grid block. Modification is done in the file such that the value of layer 19 is set to 0.0515327, the value of layer 22 is set to 0.03217513 and the value of layer 37 is set to 0.05800985. All three values of critical gas saturation is lower than the original value of 0.062.

All other input data needed to simulate is similar to the data used in the BASE CASE REF simulation run.

### **9.2 Simulation results**

The BASE CASE REF UPSC is simulated with ECLIPSE, and a visualization of the run is evaluated with FLOVIZ and S3GRAF. A 3D visualization of the grid with color scheme representing gas saturation (SGAS) is presented in Figure 9.1, and shows a comparison of gas saturation distribution at the last simulation time step (1 JAN 2025) from BASE CASE REF and BASE CASE REF UPSC.

**9 BASE CASE REF WITH UPSCALED PARAMETERS IN  
MAIN FIELD  
(BASE CASE REF UPSC)**

---

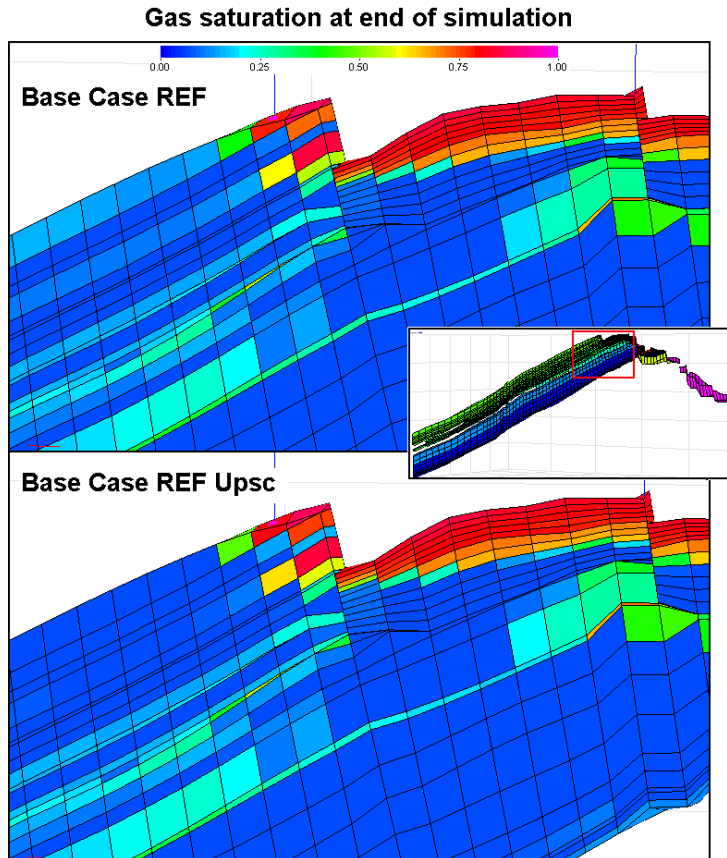


Figure 9.1: Comparison of BASE CASE REF (*top image*) and BASE CASE REF UPSC (*bottom image*) with respect to gas saturation distribution at the end of the simulations (1 JAN 2025). The color scheme represents the gas saturation. The drainage of gas in Upper Brent is observed to be much better in the upscaled model. However, little effect is observed in Lower Brent.

Investigating Figure 9.1, it is observed a much better drainage of Upper Brent gas in the BASE CASE REF UPSC simulation run. The two layers in Upper Brent which have been upscaled, are observed to have a moderate gas saturation at the end of the simulation in the BASE CASE REF simulation run, where in BASE CASE REF UPSC they are observed to have little or no gas saturation down flank. There are no visual differences observed in the gas production from Lower Brent. This observation strengthens the statement that the layer above refined zone 4 (layer 37 in BASE CASE REF) was originally adequately thin to simulate the effect, and did not need to be upscaled.

A comparison between BASE CASE REF, RMF 2 and BASE CASE REF UPSC with respect to gas production rates is presented in Figure 9.2.

9 BASE CASE REF WITH UPSCALED PARAMETERS IN  
 MAIN FIELD  
 (BASE CASE REF UPSC)

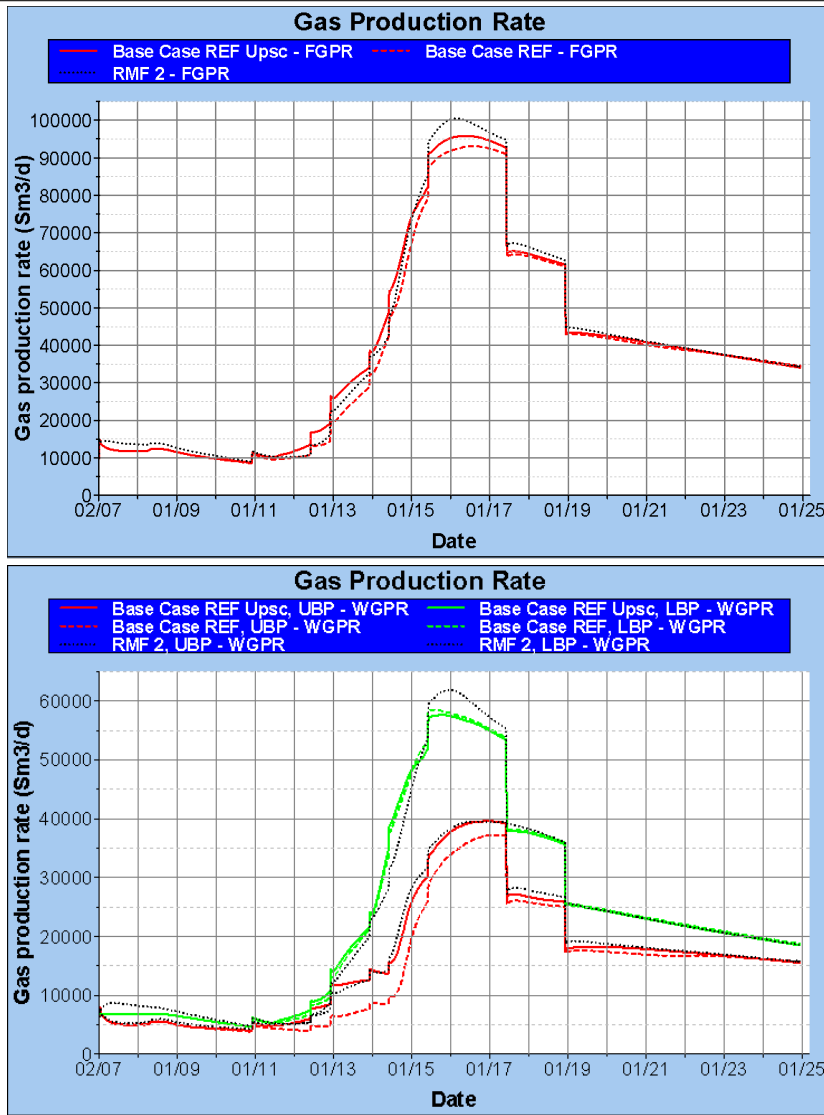


Figure 9.2: *Top plot:* The development of total gas production rate in the BASE CASE REF UPSC simulation run compared with RMF 2 and BASE CASE REF. *Bottom plot:* The development of gas production rate from each well in the BASE CASE REF UPSC simulation run compared with the RMF 2 and BASE CASE REF.

At the peak of the “gas bubble”, the upscaled model is observed to simulate a rate located in between RMF 2 and BASE CASE REF considering the total gas production rates. However, investigating the individual gas production rate the difference preventing the upscaled model to match RMF 2 originates from LBP. This is likely to be caused by the restriction observed in the layer upscaled in Lower Brent.

**9 BASE CASE REF WITH UPSCALED PARAMETERS IN  
MAIN FIELD  
(BASE CASE REF UPSC)**

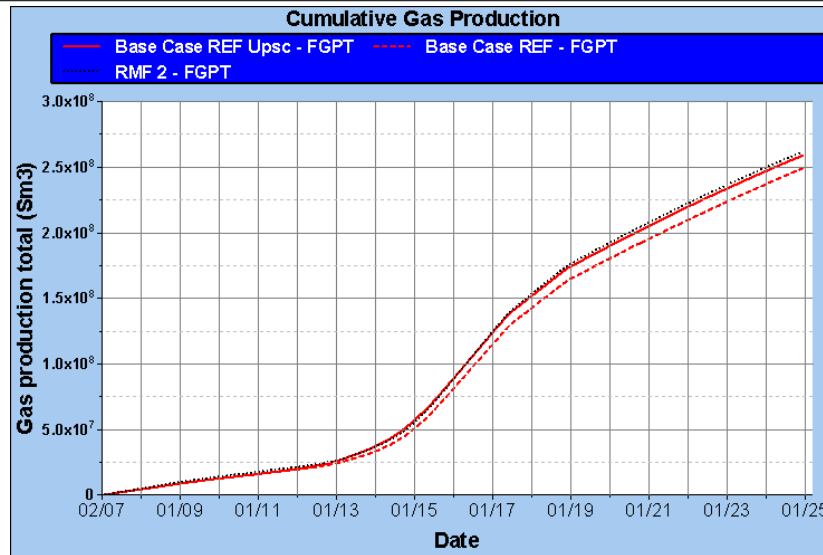


Figure 9.3: The development of total cumulative gas production in the BASE CASE REF UPSC simulation run compared with RMF 2 and BASE CASE REF. The effect of upscaling the Main Field is observed as an increased total cumulative gas production of 4 %. However, the upscaled model is observed to have a total cumulative gas production which is 1 % lower than RMF 2, caused by the restriction of a low absolute permeability cell.

Considering total gas production rates, the upscaled model is observed to have a lower value at the peak of the “gas bubble” than RMF 2. However, it will increase the value at the peak of the “gas bubble” from BASE CASE REF. If the individual gas production rate from each well in Figure 9.2 is investigated, it becomes obvious that the upscaled model matches RMF 2 in gas production rates from Upper Brent. Gas production is not increased from Lower Brent when upscaling. This yields that the gas production rate from LBP is the origin to the difference between the total gas production rates of the refined RMF 2 and the upscaled BASE CASE REF UPSC. The difference in production from Lower Brent is discussed earlier, and is likely to originate from the restriction of low absolute permeability found in a single cell in the thin, high gas mobility layer. This restriction may become negligible when 3 dimensional flow is allowed by the model, if the restriction is a local deviation.

Figure 9.3 is a comparison between BASE CASE REF, RMF 2 and BASE CASE REF UPSC with respect to total cumulative gas production. The upscaled model is observed to simulate a total cumulative gas production of  $2.59 \cdot 10^8 \text{ Sm}^3$ . This is an 4 % increase from the simulated  $2.49 \cdot 10^8 \text{ Sm}^3$  in BASE CASE REF. However, the mentioned restriction in Lower Brent is likely to cause the decrease of 1 % from the  $2.62 \cdot 10^8 \text{ Sm}^3$  simulated in RMF 2.

## 10 Further work

All simulation models investigated in this thesis are 2 dimensional, and have basis in a slice from the FFM2005 full field simulation model for the Statfjord Field. It has not been investigated any 3 dimensional effects of refining grid and upscaling relative gas permeability. However, trends like the one that gas segregates upwards until a vertical flow barrier is encountered, making thin, high gas mobility layers is still expected in a 3 dimensional case. Some of the observed 2D data will still be valid in a 3D situation.

The next step in the work of this thesis would be to investigate the effects described, for a 3D situation. Considering a 3D situation, a radial flow towards the wells with vertical 2D slices lined up perpendicular to a tangent around the center would be the best approach to describe the system. However, the Statfjord Field has a structure which implies a less complex view of the flow. The producers are located at top structure, the reservoir has a dip going ESE-WNW and has almost no dip in the perpendicular direction. This structure has caused earlier observations of the injected down flank gas with tracer to flow relatively linear along the WNW-ESE direction towards top structure, and distribute in other directions at the top structure. These observations will simplify the system describing a 3D scenario in the Statfjord Field.

The Statfjord Field can be simplified when upscaling a 3D model, and radial effects may be neglected. A proposed method is to evaluate a model similar to those created in this thesis, including 10-20 additional slices in Y-direction. Upscale with transmissibility weighted average relative gas permeability in both Y- and X-direction, and evaluate if an upscaled X-direction will describe the flow with sufficient accuracy. In addition, small effects of local restrictions, such as encountered in Lower Brent in the models of this thesis, can be evaluated. This will answer if the restriction still will force the gas flow down into underlying layers.

When a conclusion of the flow in Y-direction versus the flow in X-direction is established, it can be discussed if upscaling from a simplified small model can be applied to a larger region of the field with similar structure and properties.

When a method for upscaling the full field model is established, a further investigation of properties should be performed. All properties belonging to the coarse grid blocks in FFM2005 are average values calculated from the fine grid geological realization. In the layers below the vertical flow barriers considered in the Statfjord Field, a coarsening upwards trend favors good reservoir quality closer to the barrier. The properties from the geostatistical realization should be applied to the refined layers before a transmissibility weighted average relative gas permeability is calculated.

An upscaling of the East Flank of the Statfjord Field should also be carried out. This will be a more complex procedure, since the East Flank contains several faults. In addition to the transmissibility weighted average relative gas permeability, the way simulation of the flow across faults is calculated yields a weighting of area in contact with non-neighbor blocks.



## 11 Conclusion

Through simulation and analysis of the results it can be established a method of upscaling a 2D reservoir simulation model. However, without further simulation and analysis of a 3D scenario, it is not possible to establish if the method is adequate in a 3D scenario. All conclusions made in this thesis are considered for a 2D simulation model only. In the Statfjord Field it is still reasonable to assume that a 3D upscaling would be quite similar, assuming linear flow towards the top of the structure.

The general trend is observed to be an underestimation of gas production if a simulation model is not upscaled to include the effect of liberated gas segregating upwards until a vertical flow barrier is met. In order to adapt a simulation model to include the effect, an upscaling method is needed. The conclusions in this thesis are divided into three different topics of interest, presented in subsections 11.1, 11.2 and 11.3. The first conclusion deals with the considerations which must be handled when creating a new reservoir simulation model, while the second conclusion concerns an upscaling procedure of an already existing reservoir simulation model. At last, a conclusion considering the Statfjord Field is presented.

### 11.1 Recommendation when building a new reservoir simulation model

Through the analysis of the different simulation models, it has been established that one single, adequately thin layer is sufficient for ECLIPSE to be able to simulate the effect. It must be located directly below a vertical flow barrier. A vertical flow barrier is a layer in which the vertical transmissibility is set to zero. ECLIPSE will allow gas to segregate up into this thin layer. Considerations must be made if the velocity of liquid flow in the reservoir is relatively high, and can restrict the vertical flow of gas liberated, causing the gas to flow towards the production well together with the liquid. In a situation with high reservoir liquid flow velocity, the gas may not be able to segregate all the way up to a vertical flow barrier and create a thin, high gas mobility layer.

In the Statfjord Field, a layer is established as adequately thin if it has a height of about 2 meters. A significantly smaller amount of liberated gas will most likely not be expected. It would not be a situation where this drainage strategy would be preferred, and is a situation of theoretical value only. It has also been established that a layer with a height slightly less than 1 meter in the Statfjord Field is still able to receive all gas segregated into it. If the amount of liberated gas is expected to be significantly larger, the height must be considered for each separate situation. The height of a layer below a vertical flow barrier in a Statfjord simulation model is recommended set to 2 meters.

A simulation model for an oil reservoir with no gas cap, where a significant amount of gas liberated in the reservoir during the production period is expected, is considered. In order to include the effect of gas creating thin, high mobility layers, it is recommended to create a relatively thin layer below vertical

flow barriers to avoid later upscaling of the relative gas permeability. However, caution should be exercised if local restrictions exist in the thin layer created.

### 11.2 Upscaling an existing simulation model

Through analysis of the different simulation models, it has been established that a transmissibility weighted average relative gas permeability can be used to upscale the relative permeability. The method is not only applicable to the Statfjord Field. It can be assumed to be a method which is adequate in general. Considering an existing reservoir simulation model, a small area which is representative for a larger region is chosen. The grid is investigated to locate layers with zero transmissibility. The layer below such a vertical flow barrier has a potential of accumulating liberated gas, and create thin, high gas mobility "layers". The layer with such potential should be refined, creating an adequately thin layer below the vertical flow barrier. A simulation with refined grid is carried out, writing the required parameters belonging to the refined grid blocks in a file. The parameters are used to calculate transmissibility weighted average relative gas permeabilities and pore volume weighted average saturations. The average relative permeability is then plotted against average saturation for the flow area covered by the blocks which was refined. Assuming a normalized Corey relative gas permeability curve, the denormalized Corey relative gas permeability curve is used to create a best match to the plotted curves by using the least square method and varying the Corey exponent and critical gas saturation. From this best match, normalized Corey relative gas permeability tables are made and applied, together with critical gas saturation found, to the grid blocks which were refined in the original simulation model. This method should upscale the simulation model to predict a gas production quite similar to the refined simulation model. However, caution should be exercised if local restrictions exist in the refined layers. The Corey relative permeability tables and critical gas saturation found may be applied to the larger region represented by the small area considered when upscaling.

### 11.3 FFM2005

Considering the results of upscaling layers below a vertical flow barrier in the Statfjord Full Field Simulation Model, it becomes eminent that the original simulation model underestimates the gas production. Investigating the effect of the thin, high gas mobility layers, a refined grid is equivalent to an upscaled model. Analysis stated a 4 % increase in total cumulative gas production from  $2.49 \cdot 10^8 \text{ Sm}^3$  in BASE CASE REF to  $2.59 \cdot 10^8 \text{ Sm}^3$  in BASE CASE REF UPSC. This increase originates from the upscaling of the Main Field only. If this increase is evaluated at full field scale, it becomes a significant increase of gas reserves. If an upscaling of the East Flank is considered, the increase in gas production is equivalent with going from BASE CASE to BASE CASE REF. The upscaling of both the Main Field and The East Flank then yields an 7 % increase in total cumulative gas production from  $2.42 \cdot 10^8 \text{ Sm}^3$  in BASE CASE



to  $2.59 \cdot 10^8 \text{ Sm}^3$  in BASE CASE REF UPSC. The results are obtained from an upscaling of a 2D simulation model. If a 3D simulation is considered, the upscaling could result in both a smaller or a larger increase. Nevertheless, a significant increase in total cumulative gas production is expected, and yields an increase in gas reserves in the Stafjord Field.

**11 CONCLUSION**

---

---

## References

- [1] Dr. Ron Blakey. Mollewide plate tectonic maps. <<http://jan.ucc.nau.edu/rcb7/mollglobe.html>>.
- [2] R. Boge, S.K. Lien, A. Gjesdal, and A.G. Hansen. Turning a north sea oil giant into a gas field - depressurization of the statfjord field. *SPE 96403*, 2005.
- [3] Norwegian Petroleum Directorate. Wellbore 33/12-1. <<http://www.npd.no/engelsk/cwi/pbl/en/well/all/417htm>>.
- [4] Statfjord D&W. *Statfjord Main Completion Program*. StatoilHydro, 2008.
- [5] Hans Kleppe. *Reservoir Simulation*. University of Stavanger, 2010.
- [6] Kari N. Kulkarni, Dag Frafjord, Hilde Breivik, Kristin Helland, Eva Ø. Bjørnstad, Rune Jakobsen, Turid Ersdal, Andreas Bielinski, Morten Andreas Leonthin, Ingunn J. Kvamme, Elen W. Arnesen, Arne Egil Fylling, Tore Weltzin, and Olaf Steensland. *Annual status report 2010 for the Statfjord Field*. Statoil ASA, 2010.
- [7] Ingunn J. Kvamme. Statfjord - lithostratigraphic column for the reservoir section. Statoil ASA, Internal document.
- [8] Thomas Lerdahl, Egil B. Petersen, Alf Birger Raustad, Jan Åge Stensen, Jon Knut Ringen, Pål-Eric Øren, and Thomas G. Theting. *Preliminary Recommendations on gas-oil flowparameter for blow down on the Statfjord field*. Statoil ASA, June 2004.
- [9] Jan Inge Logstein. Ffm2005 - full field simulation models 2005. Statoil ASA, Internal document.
- [10] Rafael Osorio. Procedure in reservoir simulation. <<http://www.petrologger.com/2011/01/procedure-in-reservoir-simulation.html>>.
- [11] Schlumberger. *ECLIPSE Reference Manual 2009.2*, 2009.
- [12] Schlumberger. *ECLIPSE Technical Description 2009.2*, 2009.
- [13] Smedvig Technologies. *ResView manual*, version 5.1 edition, Dec 1998.
- [14] Egil Stangeland, Pierre Labes, Sten Viggo Lundbo, Torbjørn N. Monsen, Kristin Helland, Asle Jonassen, Erling Evensen, Hilde Breivik, Geir Løkklingholm, Synnøve Lind Rygh, Hans Christian Magelsen, and Eva Ø. Bjørnstad. *Statfjord Reservoir Development Plan 2007*. StatoilHydro, 2007.
- [15] Harald Steensland. The use of sea water tracer as a tool for history matching in the statfjord full field simulation model. Master's thesis, UiS, 2010.

## ***REFERENCES***

---

- [16] Wikipedia. Eclipse (reservoir simulator). <[http://en.wikipedia.org/wiki/ECLIPSE\\_\(reservoir\\_simulator\)](http://en.wikipedia.org/wiki/ECLIPSE_(reservoir_simulator))>, Nov 2010.
- [17] Pinggang Zhang, Gillian Pickup, and Mike Christie. A new practical method for upscaling in highly heterogeneous reservoir models. *SPE 103706*, 2007.

# APPENDIX

## A Figures and Tables

Statfjord - Lithostratigraphic column for the reservoir section

Age	Group	Formation/ subdivision	Litho- logy	Description	Dominant Colour	Occasional Colour	Depositional Environment	Depth/ Thickness
L. JUR.	Viking Group	Draupne		Claystone, organic rich, non-calcareous	black	dark grey-brown	Restricted marine, anoxic	T. Draupne Fm. 1500-2200m TVDSS 2800m TVDSS Thickness 650m
		Rew. Brent (East Flank)		Sandstone, claystone	grey	grey-brown	Gravitation. slump	
MID JURASSIC	Brent Group	Heather		Silty claystone, streaks limestone	grey		open marine	T. Brent Gp. 2333-2600m TVDSS Thickness 190-250m
		Tarbert		Sandstone, minor siltst., clayst., minor coal, limest	Grey - brown		Shoreface (retrograding) delta plain	
		Ness		Claystone, sandstone, siltstone, coal	Grey - brown		coastal plain, alluvial plain	
		Etive		Sandstone, minor coal	Grey-brown	white	Upper shoreface tidal bay	
		Rannoch		sandstone, micaceous, minor claystone, limestone	Light brown		delta front, prograding shoreface	
		Broom		Conglomeratic sandstone	Pale grey, brown		gravity flow, shallow marine	
		EARLY JURASSIC	Dunlin Group	Drake		Claystone, slightly sandy, calcareous	Medium - dark grey	
Cook				Shale, siltstone, sandstone	grey	White, grey-brown	Shallow marine, shoal sand	
Burton				Claystone	Dark grey, reddish grey		open marine	
Amundsen				Shale, siltstone, occ minor limestone at base	grey, light grey	Green, red	shallow marine	
L. TR	Statfjord Fm.			Nansen Member		Coarse sandstone	white, light grey	
		Eiriksson Member		sandstone, claystone (palaeosol)	grey, green	green-grey, red-brown	alluvial plain	
		Raude Member		claystone (palaeosol) stringers of sandstone minor dolomite	grey, red	green	alluvial plain	

Figure A.1: Lithostratigraphic overview of the Statfjord Field [7].

Lithostratigraphy		Lithostratigraphy Statfjord	Sequence Stratigraphy Statfjord	Geomodel FFM2005	Dynamic Reservoir Simulation Model FFM2005
Viking Gp	Rev. Brent	Revoiked Brent	Revoiked Brent	East Flank	East Flank
				Main Field	Main Field
Brent Gp	Tarbert Fm	Tarbert	T.6	7 - 13 (7)	7
			T.7	14 - 21 (8)	8
			T.8	22 - 29 (8)	9
			T.5	30 - 39 (10)	10
			T.4	40 - 45 (6)	11
			T.3	46 - 47 (2)	12
			T.2	48 - 51 (4)	13
			T.1	52 - 57 (6)	14
			M.10	58 - 61 (4)	15
			M.9	62 - 67 (6)	16
	Ness Fm	Ness 2	M.8	68 - 70 (3)	17
			M.7	71 - 76 (6)	18
			M.6	77 - 80 (4)	19
			M.5	81 - 84 (4)	20
			M.4	85 - 90	21
			M.3	91 - 94	22
			M.2	95 - 100	23
			M.1	101 - 116	24
				117 - 133	25
				133 - 152	26
	Etive Fm	Etive		153 - 170	27
				171 - 182	28
	Rannoch Fm	Rannoch 2		183 - 194	29
				195 - 200	30
		Rannoch 1		201 - 206	31
			207 - 213	32	
Broom Fm	Broom		214 - 224	33	
			225	34	

Figure A.2: Layer overview FFM2005 [9].

Lithostratigraphy Statfjord (Brent Gp.)	East Flank		
	FFM2005	Base Case	All other models
<b>Reworked Brent</b>	1	1	1
<b>Tarbert</b>	2	2	2
			3
			4
			5
			6
			7
<b>Ness 2</b>	3	3	8
			9
			10
			11
			12
			13
<b>Ness 1</b>	4	4	14
<b>Etive</b>			15
			16
			17
<b>Rannoch 2</b>	5	5	18
<b>Rannoch 1</b>			
<b>Broom</b>	6	6	

Figure A.3: Layer overview for the East Flank in the different 2D models. The height of the layers in the overview is not in scale with the height of the layers in the model.

A FIGURES AND TABLES

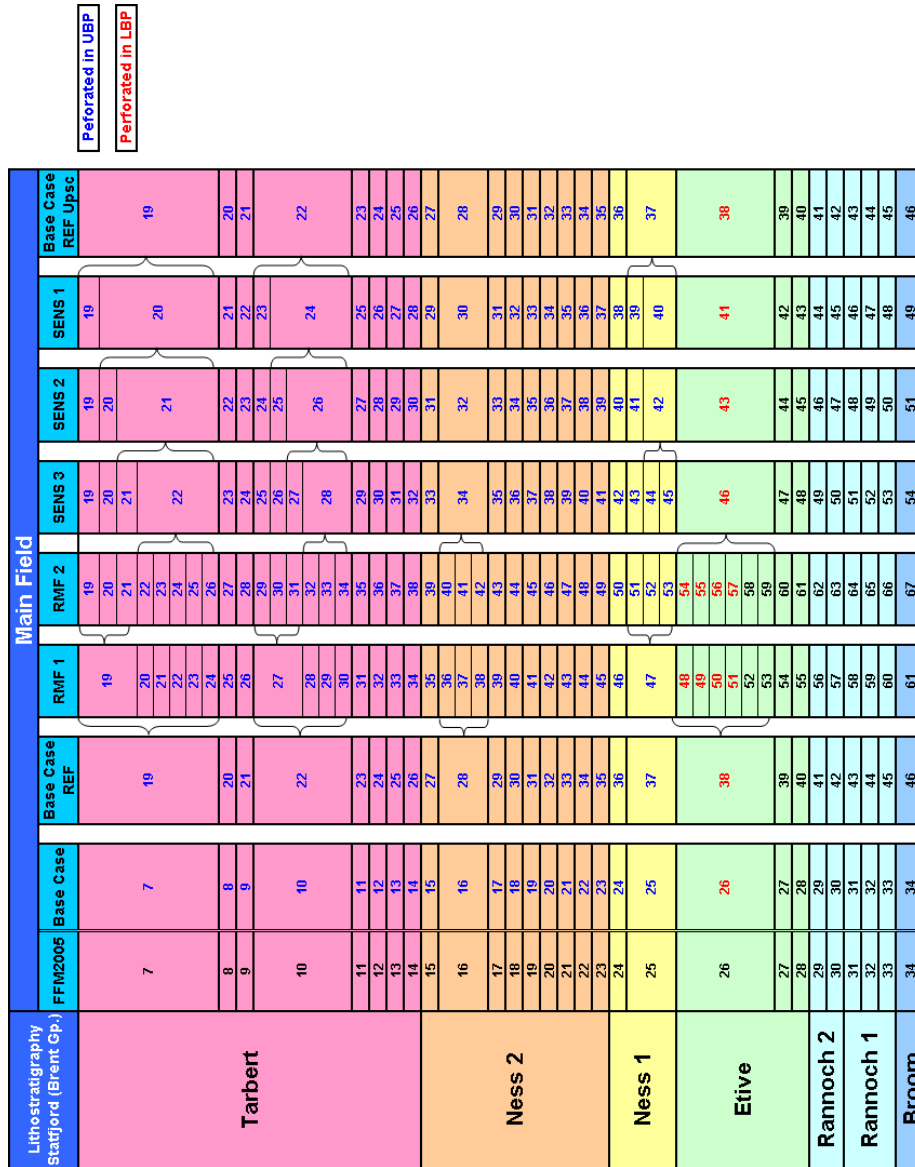


Figure A.4: Layer overview for the Main Field in the different 2D models. The height of the layers in the overview is not in scale with the height of the layers in the model.



Initial Parameters		Restart parameters
PERMX	PERMZ	PRESSURE
PORO	NTG	SWAT
SWCR	MULTX	SGAS
MULTZ	MULTPV	SOIL
SATNUM	SGU	RS
SWATINIT	SOWCR	RV
SOGCR	SGCR	
PVTNUM	EQLNUM	
ACTNUM		

Table A.1: Keywords of all parameters exported from RESVIEW to obtain input for simulation in ECLIPSE. One keyword represents a matrix containing this specific parameter belonging to all cells in the model.

**A FIGURES AND TABLES**

---

Cell selected for corey adaptment:	39 1 19-26
Swcr (base case):	0.056269
Sgc:	0.0515327
Corey exponent:	1.6724857
SUM SQ:	78.151622

<b>SGFN</b>		
SgN	Krg calc	Pc
0.000000	0.000000	0.000000
0.050000	0.006669	0.000000
0.100000	0.021258	0.000000
0.150000	0.041882	0.000000
0.200000	0.067761	0.000000
0.250000	0.098415	0.000000
0.300000	0.133504	0.000000
0.350000	0.172767	0.000000
0.400000	0.215999	0.000000
0.450000	0.263029	0.000000
0.500000	0.313712	0.000000
0.550000	0.367926	0.000000
0.600000	0.425560	0.000000
0.650000	0.486520	0.000000
0.700000	0.550717	0.000000
0.750000	0.618076	0.000000
0.800000	0.688524	0.000000
0.850000	0.761999	0.000000
0.900000	0.838439	0.000000
0.950000	0.917789	0.000000
1.000000	1.000000	0.000000

Table A.2: The normalized Corey relative gas permeability table obtained from the layers 19-26 in RMF 2 by the upscaling procedure described in subsection 1.4. The table is used for layer 19 in BASE CASE REF UPSC.

Cell selected for corey adaptment:	41 1 29-34
Swcr (base case):	0.024823
Sgc:	0.03217513
Corey exponent:	2.44311151
SUM SQ:	91.6555996

<b>SGFN</b>		
SgN	Krg calc	Pc
0.000000	0.000000	0.000000
0.050000	0.000663	0.000000
0.100000	0.003605	0.000000
0.150000	0.009707	0.000000
0.200000	0.019604	0.000000
0.250000	0.033814	0.000000
0.300000	0.052790	0.000000
0.350000	0.076932	0.000000
0.400000	0.106608	0.000000
0.450000	0.142154	0.000000
0.500000	0.183887	0.000000
0.550000	0.232101	0.000000
0.600000	0.287077	0.000000
0.650000	0.349081	0.000000
0.700000	0.418367	0.000000
0.750000	0.495177	0.000000
0.800000	0.579746	0.000000
0.850000	0.672299	0.000000
0.900000	0.773053	0.000000
0.950000	0.882219	0.000000
1.000000	1.000000	0.000000

Table A.3: The normalized Corey relative gas permeability table obtained from the layers 29-34 in RMF 2 by the upscaling procedure described in subsection 1.4. The table is used for layer 22 in BASE CASE REF UPSC.

**A FIGURES AND TABLES**

---

Cell selected for corey adaptment:	48 1 51-53
Swcr (base case):	0.093251
Sgc:	0.05800985
Corey exponent:	2.12591052
SUM SQ:	42.9903877

<b>SGFN</b>		
SgN	Krg calc	Pc
0.000000	0.000000	0.000000
0.050000	0.001714	0.000000
0.100000	0.007483	0.000000
0.150000	0.017719	0.000000
0.200000	0.032663	0.000000
0.250000	0.052490	0.000000
0.300000	0.077340	0.000000
0.350000	0.107332	0.000000
0.400000	0.142566	0.000000
0.450000	0.183131	0.000000
0.500000	0.229106	0.000000
0.550000	0.280566	0.000000
0.600000	0.337574	0.000000
0.650000	0.400194	0.000000
0.700000	0.468481	0.000000
0.750000	0.542490	0.000000
0.800000	0.622269	0.000000
0.850000	0.707866	0.000000
0.900000	0.799326	0.000000
0.950000	0.896690	0.000000
1.000000	1.000000	0.000000

Table A.4: The normalized Corey relative gas permeability table obtained from the layers 51-53 in RMF 2 by the upscaling procedure described in subsection 1.4. The table is used for layer 37 in BASE CASE REF UPSC.

## B Example of an ECLIPSE \*.DATA file

```
--INITIAL ATTEMPT ON UPSCALING ON SLICE 43 Y-DIRECTION
RUNSPEC
TITLE
SIM 1 SLICE 43 Y-DIRECTION
DIMENS
111 1 34 /
START
1 FEB 2007 /
GRIDOPTS
YES /
OIL
GAS
WATER
DISGAS
VAPOIL
METRIC
SATOPTS
'DIRECT' /
ENDSCALE
'NODIR' 'REVERS' 1 20 /
--EQLOPTS
-- 'MOBILE' 'THPRES' /
ACTDIMS
40 100 100 5 /
TABDIMS
-- NTSFUN NTPVT NSSFUN NPPVT NTFIP NRPVT
11 2 30 24 55 20 /
EQLDIMS
3 100 20 /
REGDIMS
-- NTFIP NMFIPR NRFREG NTFREG
59 3 0 100 /
FAULTDIM
1000 /
WELLDIMS
5 50 2 5 /
VFPPDIMS
20 20 15 15 15 50 /
AQUDIMS
-- AQUNUM AQUCON
250 150 /
NUPCOL
1 /
SMRYDIMS
30000 /
UNIFIN
UNIFOUT
MEMORY
1000 /
-- NOSIM
MESSAGES
-- Message Comment Warning Problem Error Bug
-- print limit
5000 5000 10000 100 100 100
--stop limit
100000 100000 100000 100000 100 10
/
-- *****
GRID
INIT
NEWTRAN
MAPAXES
0.0 100.0 0.0 0.0 100.0 0.0 /
INCLUDE
'/project/stf2008/SF_UNIT/SF_FF/UPSCALING/BRENT/INCLUDE_1/SLICE.GRDECL' /
INCLUDE
```

## B EXAMPLE OF AN ECLIPSE \*.DATA FILE

---

```

'/project/stf2008/SF_UNIT/SF_FF/UPSCALING/BRENT/INCLUDE_1/poro.dat' /
INCLUDE
'/project/stf2008/SF_UNIT/SF_FF/UPSCALING/BRENT/INCLUDE_1/ntg.dat' /
INCLUDE
'/project/stf2008/SF_UNIT/SF_FF/UPSCALING/BRENT/INCLUDE_1/permx.dat' /
INCLUDE
'/project/stf2008/SF_UNIT/SF_FF/UPSCALING/BRENT/INCLUDE_1/permz.dat' /
COPY
PERMX PERMY /
/
-- Volume fix
INCLUDE
'/project/stf2008/SF_UNIT/SF_FF/UPSCALING/BRENT/INCLUDE_1/multpv.dat' /
INCLUDE
'/project/stf2008/SF_UNIT/SF_FF/UPSCALING/BRENT/INCLUDE_1/multz.dat' /
INCLUDE
'/project/stf2008/SF_UNIT/SF_FF/UPSCALING/BRENT/INCLUDE_1/fluxnum.dat' /
GRIDFILE
1 0 /
MINPV
200 /
PINCH
0.1 'GAP' /
GRIDUNIT
METRES /
-- *****
EDIT
-- value of TRANZ must not exceed 5000
MAXVALUE
'TRANZ' 5000 1 111 1 1 1 34 /
/
-- *****
PROPS
INCLUDE
'/project/stf2008/SF_UNIT/BASE_2005/INCLUDE/BRENT/PROPS/gipvt_cpcw50_dec2002_nh.97' /
-- (PVTG, PVT0, PVTW, ROCK, DENSITY)
INCLUDE
'/project/stf2008/SF_UNIT/SF_FF/UPSCALING/BRENT/INCLUDE_1/STF_SGFN_PRED_WAG.relp' /
-- (SGFN)
INCLUDE
'/project/stf2008/SF_UNIT/HISTORY/WORK_HIST_BRENT/BEST/INCLUDE/STF_SWFN_PRED_WAG.relp' /
-- (SWFN)
INCLUDE
'/project/stf2008/SF_UNIT/HISTORY/WORK_HIST_BRENT/BEST/INCLUDE/STF_SOF3_PRED_WAG.relp' /
-- (SOF3)
INCLUDE
'/project/stf2008/SF_UNIT/SF_FF/UPSCALING/BRENT/INCLUDE_1/swatinit.dat' /
INCLUDE
'/project/stf2008/SF_UNIT/SF_FF/UPSCALING/BRENT/INCLUDE_1/swcr.dat' /
INCLUDE
'/project/stf2008/SF_UNIT/SF_FF/UPSCALING/BRENT/INCLUDE_1/sgu.dat' /
INCLUDE
'/project/stf2008/SF_UNIT/SF_FF/UPSCALING/BRENT/INCLUDE_1/sogcr.dat' /
INCLUDE
'/project/stf2008/SF_UNIT/SF_FF/UPSCALING/BRENT/INCLUDE_1/sowcr.dat' /
COPY
'SWCR' 'SWL' /
/
EQUALS
KRO 1.000 1 111 1 1 1 34 /
KRW 0.800 1 111 1 1 1 34 /
/
INCLUDE
'/project/stf2008/SF_UNIT/SF_FF/UPSCALING/BRENT/INCLUDE_1/sgcr.dat' /
-- *****
REGIONS
EQUALS
'KRNUMZ' 11 1 111 1 1 25 34 /
```

---

**B EXAMPLE OF AN ECLIPSE \*.DATA FILE**

---

```
'KRUNUMZ' 11 1 111 1 1 4 5 /
/
INCLUDE
'/project/stf2008/SF_UNIT/SF_FF/UPSCALING/BRENT/INCLUDE_1/pvtnum.dat' /
INCLUDE
'/project/stf2008/SF_UNIT/SF_FF/UPSCALING/BRENT/INCLUDE_1/satnum.dat' /
INCLUDE
'/project/stf2008/SF_UNIT/SF_FF/UPSCALING/BRENT/INCLUDE_1/fipnum.dat' /
-- *****
SOLUTION
INCLUDE
'/project/stf2008/SF_UNIT/SF_FF/UPSCALING/BRENT/INCLUDE_1/pressure.rst' /
INCLUDE
'/project/stf2008/SF_UNIT/SF_FF/UPSCALING/BRENT/INCLUDE_1/sgasedt.rst' /
INCLUDE
'/project/stf2008/SF_UNIT/SF_FF/UPSCALING/BRENT/INCLUDE_1/swat.rst' /
INCLUDE
'/project/stf2008/SF_UNIT/SF_FF/UPSCALING/BRENT/INCLUDE_1/rs.rst' /
INCLUDE
'/project/stf2008/SF_UNIT/SF_FF/UPSCALING/BRENT/INCLUDE_1/rv.rst' /
SUMMARY
INCLUDE
'/project/stf2008/SF_UNIT/SF_FF/UPSCALING/BRENT/INCLUDE_1/summary.smr' /
-- *****
SCHEDULE
RPTSCHED
'NEWTON=1' 'WELLS=2' 'FIP=2' /
RPTRST
BASIC=2 /
INCLUDE '/project/stf2008/SF_UNIT/BASE_2005/INCLUDE/BRENT/SCHEDULE/Brent_Lift_2000_Ecl.txt' /--33
TUNING
1.0 5. 0.01 0.015 2.0 0.1 0.1 1.25 /
0.1 0.001 1.0E-07 0.0001 1.0E+01 0.01 1.0E-06 0.001 0.025 /
12 1 40 1 25 25 /
INCLUDE
'/project/stf2008/SF_UNIT/SF_FF/UPSCALING/BRENT/INCLUDE_1/schedule.sch' /
END
```